
Optimal Scheduling of Power Consumption in Green Smart Houses

Master Thesis
Robert-Octavian Popescu

Aalborg University
Electronics and IT

Copyright © Aalborg University 2017

Here you can write something about which tools and software you have used for typesetting the document, running simulations and creating figures. If you do not know what to write, either leave this page blank or have a look at the colophon in some of your books.



Electronics and IT
Aalborg University
<http://www.aau.dk>

AALBORG UNIVERSITY
STUDENT REPORT

Title:

Optimal Scheduling of Power
Consumption in Green Smart Houses

Theme:

Control and Automation

Project Period:

Spring Semester 2017

Project Group:

CA1033

Participant(s):

Robert-Octavian Popescu

Supervisor(s):

Tom S. Pedersen
Kirsten M. Nielsen
Rasmus Pedersen

Copies: 1

Page Numbers: 68

Date of Completion:

September 26, 2017

Abstract:

Due to the high growth in renewable energy generation, more and more renewable systems are being manufactured for household usage. Integrating PV system accompanied with energy storage would permit households to completely disconnect from the grid. One of the biggest consumer in a building is the heating system. This work focuses on representing a complex system composed of: house, heating, battery, PV system, backup generator. Moreover, it is investigated the efficient energy usage of the heating system in a basic house. Model predictive control (MPC) is used to fully integrate the current state of the system and the weather forecast. Moreover, minimizing the use of the backup generator in the case of insufficient power is pursued, consequently the usage of fossil fuels is reduced. Also, the predictive controller commands: heating of the house, energy storage and backup generation, thus keeping the house temperatures within comfort limits. Finally, a MPC strategy is implemented and verified through simulations.

The content of this report is freely available, but publication (with reference) may only be pursued due to agreement with the author.

Contents

Preface	vii
1 Introduction	1
1.1 Motivation	1
1.2 Literature	2
1.3 Green Smart House	3
1.4 GSH Case Study	4
2 Modeling	7
2.1 House Dynamics	7
2.2 PV System	15
2.3 Energy Storage	18
2.4 Discrete Models	19
3 Optimization	23
3.1 Objective Function	24
3.2 Constraints	26
3.3 Problem Variables	27
3.4 Model Predictive Control	29
3.5 Convex Optimization	32
4 Simulation	37
4.1 Preliminary Example	39
4.2 Battery Example	42
4.3 Scenario Comparison	46
5 Conclusion	53
Bibliography	55
A CVX-Matlab Implementation	57

B	House Dynamic Model	63
B.1	Transfer Matrix	63
B.2	Poles and Time Constants	66
B.3	Step Response	67

Preface

Aalborg University, September 26, 2017

Robert-Octavian Popescu
<popescu.robert.octavian@gmail.com>

Chapter 1

Introduction

In this chapter a short motivation will be presented, after which we will look into the literature relevant to this study, followed by describing the green smart house (GSH) concept and providing a case study example. Next the modeling of the system will be done in Chapter 2 while the optimization will be handled in Chapter 3. Further on, simulations and results will be presented in Chapter 4, and finally the conclusions of this project will be drawn in Chapter 5.

1.1 Motivation

In the last two decades there has been a high growth in renewable energy production, such that more renewable equipment systems are being manufactured for consumers households. By choosing "green energy" sources consumers can support the development of clean energy that will reduce the environmental impacts associated with conventional energy generation and increase energy independence. Moreover, these technologies can help houses by reducing bills for different utilities on a mid-long term basis. Energy systems technologies have reached to a point that they can be reliable as standalone systems, hence pushing towards a decentralization of the energy market.

In this sense, a house equipped with such a system accompanied by energy storage would provide the energy needed for daily consumption. But, there will be situations when there will not be enough energy to provide to the house due to weather circumstances. In most cases, a solution is to have a backup generator running on fossil fuels that will provide energy in the situation described previously. Another solution would be to schedule some of the devices in such a manner that will avoid using the backup generator, or draining the whole battery. Additionally, the applicability of such a scheduling system would provide optimization of energy consumption, but also it can be extended to other fields of study.

This thesis will focus on optimizing the GSH by scheduling the household consumption when green energy is available, using the backup generator as little as possible. Moreover, it will undertake the process of building the system model and finding a proper optimization method. Furthermore, the implementation of the models and optimization method will be pursued, followed by a presentation of the findings.

1.2 Literature

Nowadays, the environmental issues are more and more alarming as: *"primarily the burning of fossil fuels and deforestation caused by industry and urbanization—is responsible for a sharp and continuing rise in the concentration of carbon dioxide (CO₂)"* [16]. Thus, the energy generated by means of burning fossil fuels must come to an end.

An alternative to these solutions is the well known renewable energies: solar, wind and hydro. In [6] a simulation framework has been developed, where some renewable energy systems are described, for example: wind and solar power plants. Moreover, in the same study the description of an energy storage model is provided.

Further, in [8] the authors undergo an optimization (using Matlab's `linprog` function) by exploiting weather forecast and energy prices in conjunction with prediction models of house dynamics and floor heating systems using heat pumps. Also, it is shown the possibility to move substantial amount of energy from one time to another, whilst keeping the inhabitants within their comfort zone. Another approach is followed in [4], where model predictive control (MPC) is used to control heating and cooling of a simple house. Moreover, the predictive controller takes into account the current thermal conditions of the house and 1-day-ahead weather forecast. A different approach is taken in [15] that aims to predict the energy consumption of a residential thermal HVAC model. Such that, a second-order thermal model of the house is built in Matlab, while GridLAB-D is used to control the HVAC based on temperature, time and occupancy pattern.

In [3] a solution to the scheduling problem of smart home appliances using mixed-integer programming (MIP) is proposed. The goal, given in a load demand profile, is to minimize electricity cost fulfilling duration, energy requirement, and user preference constraints. Additionally, this study shows that by adding a PV system in a home this would result in energy bills reduction. Another scheduling approach is tackled in [1], where the study concerns optimal scheduling of a set of house appliances taking into account costs, comfort level and time. Such that, using a mixed-integer linear programming (MILP) model and a heuristic algorithm that accounts for a typical household with solar panels and energy storage. On the other hand, in [7] the authors formulate an optimization to schedule electrical

loads given short term prediction of time-varying power production, using an MPC approach with constraints, to store a limited amount of energy in the battery.

In this work, a different approach has been taken for the purpose of optimizing energy and reducing fossil fuels consumption when combining different systems such as: solar panels, energy storage, backup generator and heating system. This was achieved by having the aforementioned studies as basis and inspiration.

1.3 Green Smart House

Along this section an explanation of what is the Green Smart House (GSH), what utility it provides and how it can be used further, is given. Moreover, going through the literature discussed in 1.2, one can observe that a different approach is taken in the work at hand.

Further on, assuming that the energy provided to a GSH should rely mostly on renewable energies (solar panels, wind/hydro turbine or other). In most cases these renewable energies are somewhat limited due to natural causes (e.g. clouds blocking the sun, not enough wind). Such that, in order to be self-sustainable in an “off-grid” scenario, the green smart house system (GSHS) is defined with the following components:

- *House* with defined parameters that relate to its construction.
- *HVAC system* that provides heating to the house.
- *PV system* that generates power depending on weather conditions.
- *Battery* that stores the power from the *PV system* for later usage.
- *Backup generator* used when insufficient power is not provided to *HVAC*.

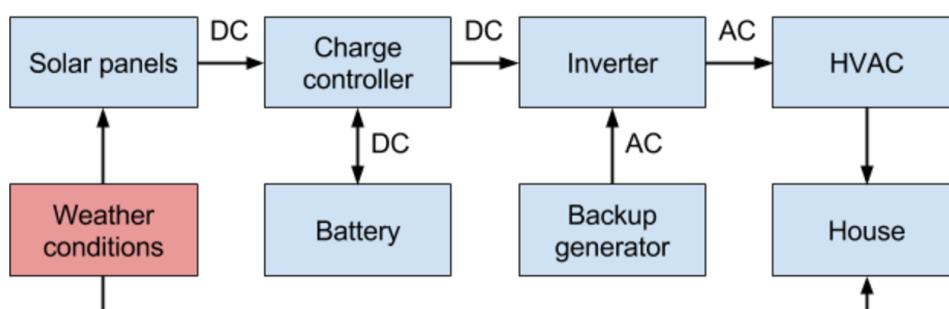


Figure 1.1: GSHS diagram. How the individual systems within the GSHS, such as solar panels, backup generator, HVAC and battery, relate and cooperate.

Furthermore, the block diagram of how the GSHS would look in a realistic scenario can be seen in Figure 1.1. Given the weather conditions the solar panels would generate power, while the charge controller would decide if the power would be stored in the battery or served to the heating system (HVAC) for providing heat to the house. Moreover, in the case of insufficient power the backup generator would provide the power shortage to the HVAC in order to keep the house temperature at a certain comfort level.

1.4 GSH Case Study

In this section a case study will be presented, and establish some basic assumptions regarding some of the house parameters and HVAC. Such that, let us consider the following house plan depicted in Figure 1.2, having a total area of $120m^2$ with 6 spaces, 7 doors (depicted in blue, 2 of them communicating to the outside and 5 inside) and 10 windows (depicted in orange). Moreover, all of these house components will impact to some extent the performance of the house, in particular the indoor temperature and consequently the overall energy consumption.

An important factor in modeling a house is knowing the thermal resistances of roof, walls, floors, windows and doors. To give an example, a house with poor insulation will be problematic since the indoor temperature will fluctuate more frequently. From a control point of view this would make it harder to schedule the heating system. To give a comparison for the house parameters one can take the examples of a poor (GSH1), average (GSH2) and good (GSH3) house insulation chosen regarding the International Energy Conservation Code in [11] and translated to SI units. The respective parameters shall be used later on in simulations to provide a comparison. In Table 1.1 the thermal resistance values of each structure of the house regarding different thermal integrity levels can be seen.

GSH	Roof $[\frac{Km^2}{W}]$	Wall $[\frac{Km^2}{W}]$	Floor $[\frac{Km^2}{W}]$	Door $[\frac{Km^2}{W}]$	Window $[\frac{Km^2}{W}]$	Level
1	2.64	0.88	0.88	0.53	0.14	Bad
2	5.28	1.94	3.34	0.59	0.30	Medium
3	8.45	3.34	3.87	0.88	0.37	Good

Table 1.1: House parameters based on different types of insulation

The heating, ventilation and air conditioning (HVAC) considered for this study uses an electric ON/OFF heat pump [2]. First, the efficiency of the heat pump is defined as the coefficient of performance (COP), which is determined by the ratio between energy usage of the compressor and useful heat extracted from the condenser in the case of a heat pump. Choosing a high COP value represents high efficiency of the heat pump. Another important aspect of the HVAC is to specify the heating setpoint which will be $21^{\circ}C$ and the deadband $\pm 3^{\circ}C$. An

important safety measure is the time limitation between ON and OFF cycles which is considered 15 minutes in this case. Control of house heating will be made based on weather forecast and PV generation.

This study will pursue to aggregate all the components presented in Section 1.3 as one self-sustainable system defined as the *GSHS*. In order to achieve this, modeling of each component will be done beforehand in Chapter 2. Afterwards, integration, controlling and optimizing the GSHS will be presented in Chapter 3. Last but not least, the results achieved in this study will be highlighted through simulations, based on a Matlab and CVX implementation Appendix A, explained in Chapter 4.

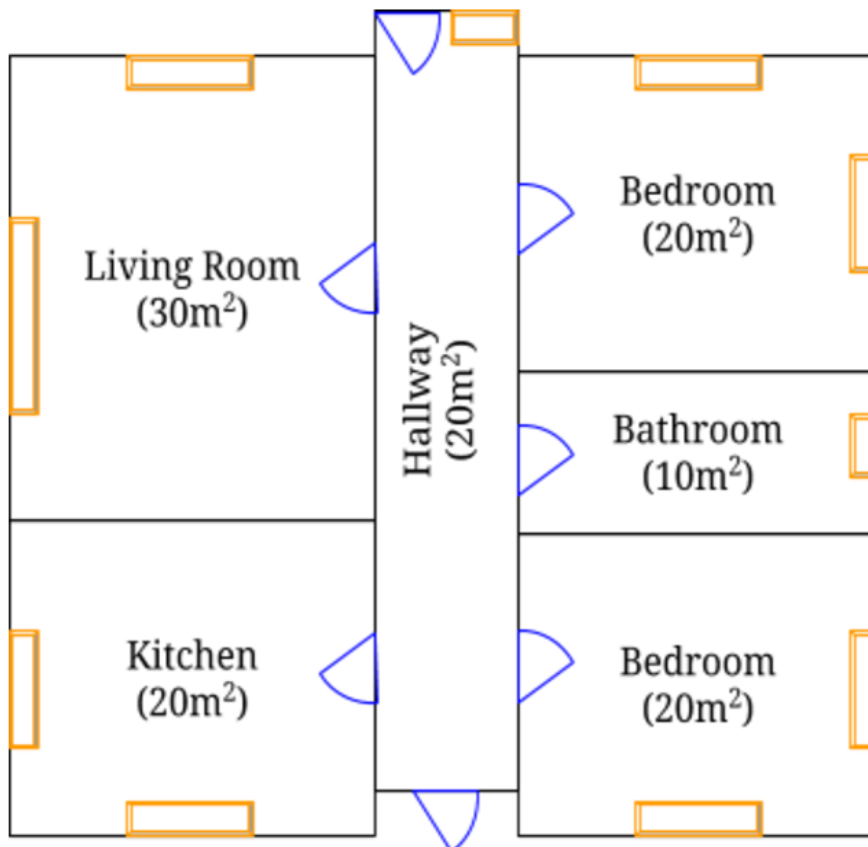


Figure 1.2: Example of GSH plan with: a total area of $120m^2$ with 6 spaces, 7 doors (depicted in blue, 2 of them communicating to the outside and 5 inside) and 10 windows (depicted in orange).

Chapter 2

Modeling

The modeling chapter defines the theoretical background of the green smart home system (GSHS) components, such that a house dynamic model is built in Section 2.1, the PV system is defined in 2.2, while the energy storage is provided in 2.3. Afterwards, discretizing all the components and forming the GSHS will be done in Section 2.4 which will be used further for the optimization presented in Chapter 3.

2.1 House Dynamics

Earlier, in Section 1.3 the house description has been made, such that in this part the heat transfer processes using resistance-capacitance equivalent models (RC networks) are presented, for details see [22]. For this house model an abstraction has been made, such that all the rooms in the house will be represented as one room with a single air T_A and mass T_M temperature. Moreover, the house parameters (U_A, U_M, C_A, C_M) relate to the materials and construction of the house as described in [18]. Knowing this, in Figure 2.1 the equivalent thermal resistance circuit of the house is shown, where:

- $T_O[^\circ\text{C}]$ - outdoor air temperature.
- $T_A[^\circ\text{C}]$ - house air temperature.
- $T_M[^\circ\text{C}]$ - house mass temperature.
- $Q_A[\text{W}]$ - heat transfer from HVAC.
- $Q_R[\text{W}]$ - heat transfer from solar radiation added directly to the room mass, bypassing air medium.
- $U_M[\text{W}/^\circ\text{C}]$ - house mass surface conductance (ceilings, interior walls and exterior walls).

- $U_A [W/^\circ C]$ - house envelope conductance (walls, windows, doors, floor and ceiling).
- $C_M [J/^\circ C]$ - house thermal mass capacitance.
- $C_A [J/^\circ C]$ - house air thermal capacitance.

Based on the study found in [8] the heat transfer from the HVAC system Q_A will be considered to be equal to the power provided P_H multiplied with a constant COP factor as in Equation (2.1).

$$Q_A(t) = COP \cdot P_H(t) \quad (2.1)$$

As discussed earlier the house thermal performance is based on a reduced equivalent thermal parameter (ETP) model in which parallel heat flow paths and series thermal mass elements are lumped into a few parameters and portrayed as a basic DC electric circuit as in Figure 2.1. Such that, by looking at the circuit in Figure 2.1 the heat balance on the indoor air temperature node T_A can be derived in Equation (2.2), whilst in (2.3) the heat balance on mass temperature node T_M can be observed. These equations describe the thermal performance of the house model. Hence, a realistic analysis can be made under changeable circumstances such as weather conditions in this case the outdoor temperature T_O and heat gain from solar radiation Q_R , but also the heat transfer from the heating system (HVAC) Q_A .

For a better understanding one can follow Equations (2.2) and (2.3) with Figure 2.2 where the heat gains/losses of the house are shown. Thus, for the air medium T_A one can observe the heat gain from the heating system Q_A , while the

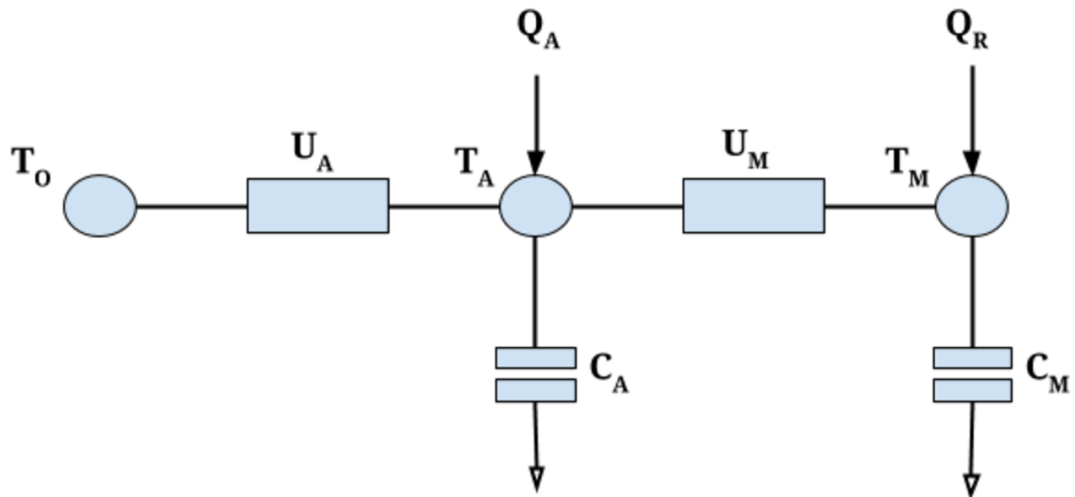


Figure 2.1: Equivalent thermal parameter (ETP) circuit of the house model.

heat gains/losses towards the house mass Q_{AM} and outdoor temperature Q_{AO} are determined by the difference in temperature between each of the media. Regarding the mass medium T_M , the main gain is the solar radiation Q_R , whilst the heat flow towards the air medium is identified as Q_{MA} . Moreover, the use of the air C_A and mass C_M capacitances is to realistically dampen the effect of the difference in temperature between each media, the heat sent from the heating system Q_A and by the solar radiation Q_R respectively. These matters are important, because they directly impact the energy consumption of the house and need to be taken into account. Hence, the house dynamics are essential to compute the air T_A and mass T_M temperatures in order to predict the amount of power P_H that needs to be provided to the HVAC system, thus keeping the house temperature within an appropriate comfort interval.

$$\underbrace{COP \cdot P_H(t)}_{Q_A} - \underbrace{U_A[T_A(t) - T_O(t)]}_{Q_{AO}} - \underbrace{U_M[T_A(t) - T_M(t)]}_{Q_{AM}} - C_A \dot{T}_A(t) = 0 \quad (2.2)$$

$$Q_R(t) - \underbrace{U_M[T_M(t) - T_A(t)]}_{Q_{MA}} - C_M \dot{T}_M(t) = 0 \quad (2.3)$$

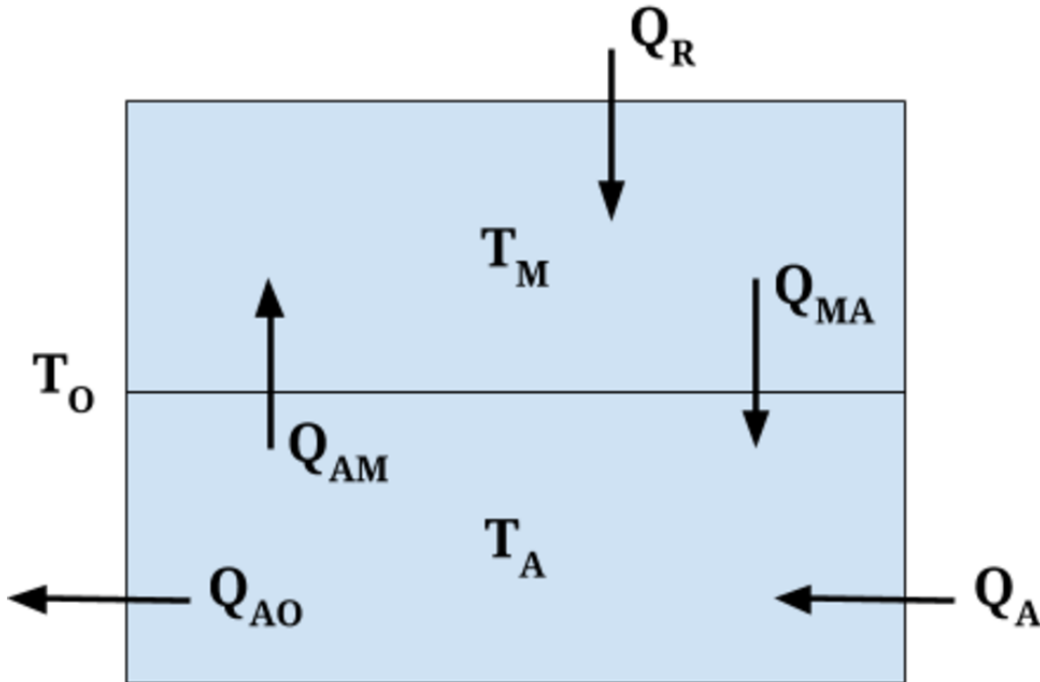


Figure 2.2: Schematic of heat flows between each media within the house.

Going forward, rewriting Equation (2.2) for the heat balance on the air temperature node T_A in the form of (2.4) and (2.3) for the mass temperature node T_M as (2.5).

$$\dot{T}_A(t) = \frac{1}{C_A}[-(U_A + U_M)T_A(t) + U_M T_M(t) + COP \cdot P_H(t) + U_A T_O(t)] \quad (2.4)$$

$$\dot{T}_M(t) = \frac{1}{C_M}[U_M T_A(t) - U_M T_M(t) + Q_R(t)] \quad (2.5)$$

State-space model

Further, using Equations (2.4) and (2.5) and arranging them in the continuous time-invariant state-space model representation having the general form as in (2.6).

$$\begin{aligned} \dot{x}(t) &= Ax(t) + Bu(t) \\ y(t) &= Cx(t) \end{aligned} \quad (2.6)$$

- x is the state vector in (2.7), $x \in \mathbb{R}^{2 \times 1}$

$$x(t) = [T_A(t) \quad T_M(t)]^T \quad (2.7)$$

- u is the input or control vector in (2.8), $u \in \mathbb{R}^{3 \times 1}$

$$u(t) = [P_H(t) \quad Q_R(t) \quad T_O(t)]^T \quad (2.8)$$

- y is the output vector in (2.9), $y \in \mathbb{R}^{2 \times 1}$

$$y(t) = [T_A(t) \quad T_M(t)]^T \quad (2.9)$$

- A is the system matrix in (2.10), $A \in \mathbb{R}^{2 \times 2}$

$$A = \begin{bmatrix} -\frac{U_A + U_M}{C_A} & \frac{U_M}{C_A} \\ \frac{U_M}{C_M} & -\frac{U_M}{C_M} \end{bmatrix} \quad (2.10)$$

- B is the input matrix in (2.11), $B \in \mathbb{R}^{2 \times 3}$

$$B = \begin{bmatrix} \frac{COP}{C_A} & 0 & \frac{U_A}{C_A} \\ 0 & \frac{1}{C_M} & 0 \end{bmatrix} \quad (2.11)$$

- C is the output matrix in (2.12), $C \in \mathbb{R}^{2 \times 2}$

$$C = \begin{bmatrix} 1 & 0 \\ 0 & 1 \end{bmatrix} \quad (2.12)$$

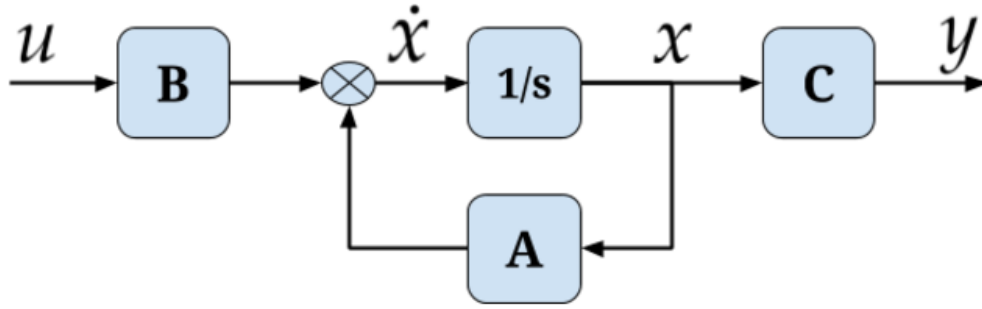


Figure 2.3: Block diagram representation of the linear state-space in Equation (2.6).

For a better understanding of the state-space given in Equation (2.6) the block diagram representation of the system is depicted in Figure 2.3, where the corresponding terms are given in Equations (2.7) - (2.12). Moreover, this shows how the input u changes the current state of the system x which will yield the output y at a given time instance.

System poles and time constants

Following the investigation of the transfer function matrix in Appendix B, further analysis of the system poles can be made, first by finding the roots of Equation (2.13), where the coefficients of each term can be found in (2.14)-(2.16).

$$as^2 + bs + c = 0 \quad (2.13)$$

$$a = 1 \quad (2.14)$$

$$b = \frac{C_M(U_A + U_M) + C_A U_M}{C_A C_M} \quad (2.15)$$

$$c = \frac{U_A U_M}{C_A C_M} \quad (2.16)$$

Knowing that all the parameters in Equation (2.18) have positive values and that the mass conductance U_M is larger than the air U_A , implies that the discriminant Δ is positive which means that the roots will be real numbers.

$$r_{1,2} = \frac{-b \pm \sqrt{\Delta}}{2a} \quad (2.17)$$

$$\begin{aligned} \Delta &= b^2 - 4ac \\ &= \frac{(U_A + U_M)^2}{C_A^2} + \frac{U_A^2 U_M^2}{C_A^2 C_M^2} + 2 \frac{U_M(U_M - U_A)}{C_A C_M} > 0 \end{aligned} \quad (2.18)$$

Now, using Equation (2.17) and knowing the house parameters, the roots can be calculated in (2.19). Moreover, using these roots factorization of Equation (2.13) can be done in (2.20), such that it can be remarked that the eigenvalues of the system are negative real values which means that the system is asymptotically stable as time evolves.

$$r_{1,2} = -\frac{C_M(U_A + U_M) + C_A U_M}{2C_A C_M} \pm \sqrt{\frac{(U_A + U_M)^2}{C_A^2} + \frac{U_A^2 U_M^2}{C_A^2 C_M^2} + 2\frac{U_M(U_M - U_A)}{C_A C_M}} \quad (2.19)$$

$$as^2 + bs + c = (s + r_1)(s + r_2) = (s + 13.506)(s + 0.114) \quad (2.20)$$

In the case of the thermal system at hand the time constants are at most important since they are directly connected with how fast the mediums cool or warm under the influence of external factors. Such that, using Equation (2.21) we can isolate the terms and find the time constants τ_1 and τ_2 found in (2.22) and (2.23). Moreover, by looking at the time constants values it can be said that τ_1 relates to the capacity of the air inside the house, whilst τ_2 describes the time needed for the house mass to cool/warm.

$$(s + r_1)(s + r_2) = \tau_1 \tau_2 \left(\frac{1}{\tau_1} s + 1\right) \left(\frac{1}{\tau_2} s + 1\right) \quad (2.21)$$

$$\tau_1 = \frac{1}{r_1} = 0.074 \quad [hours] \quad (2.22)$$

$$\tau_2 = \frac{1}{r_2} = 8.772 \quad [hours] \quad (2.23)$$

As a remark it can be said that in a realistic scenario, for example when opening a window, the room air temperature would take more or less the same time in order to cool/warm as described by the time constant τ_1 (≈ 4.5 minutes). Further, we shall assume that there are local controllers that will keep the air temperature T_A near the desired set-point.

Given the fact that the large capacity of the house mass leads to slower changes in temperature T_M , this enables heat storage for longer periods. In this case, it is more of interest to look at the time constant τ_2 when choosing the sampling time T_s . A best practice for choosing the sampling time, in this situation, would be at least 20 times the time constant as shown in Equation (2.24). Such that, a sampling period of 15 minutes shall be used further on, in finding the discrete model discussed in Section 2.4 and the simulations to come.

$$T_s \leq 0.05\tau_2 \quad (\approx 26 \text{ minutes}) \quad (2.24)$$

House model comparison and verification

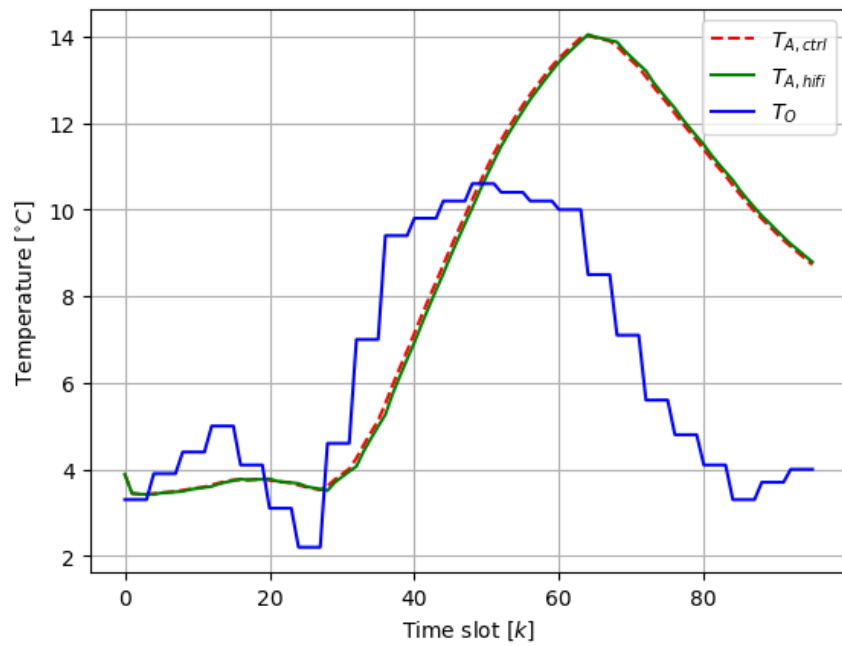
As a verification step, a model comparison of the house has been made with a similar implementation used within a well-known system simulation tool, GridLAB-D [19]. Thus, the comparison between the model within GridLAB-D tool and the control model will be presented in order to confirm the implementation of the house dynamics. To be noted that, the GridLAB-D house model is limited, but it is fairly reliable since it is used in most research studies. For more insight on how the house dynamics are implemented within this simulation tool refer to [23].

Furthermore, the house dynamic model relies on the weather data in order to compute the indoor temperature T_A . Such that, both models have the same house parameters and weather data provided by the climate module in [17] composed of: the outdoor temperature T_O and solar radiation Q_R parameters. Moreover, the climate data includes parameters as temperature, humidity, and solar radiation, which are used to calculate temperature gain that is the result of heat gained from direct exposure of a surface to sunlight. On top of that, for determining the solar radiation the model taking into account the change in tilt of the Earth polar axis with respect to the plane of the orbit around the sun through the year based on [13].

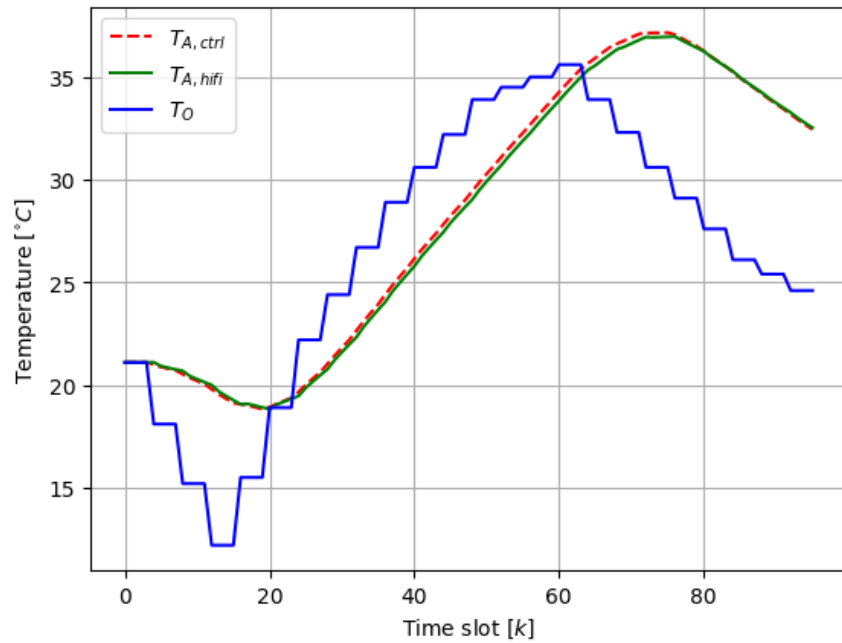
The house dynamics presented in this section has been implemented using Matlab, as provided in Appendix A. Two different scenarios have been built in order to be analysed: winter in Figure 2.4a and summer in 2.4b, where $T_{A,ctrl}$ is the indoor temperature of the current implementation whilst $T_{A,hifi}$ is the one provided by GridLAB-D.

For example, in Figure 2.4a the simulation starts off with the same indoor T_A and outdoor T_O temperatures, around $3 - 4^\circ\text{C}$, and near sample 30 (equivalent to hour 7:00, when the sun would come up) the outdoor temperature also starts to rise. After a while, the temperature in the house starts to change due to the solar radiation and ambient temperature. Also, it can be seen that the change in the indoor temperature does not occur instantly which would be the case in reality due to house insulation. Moreover, the room temperature exceeds the ambient, with almost 4°C , since the heat is stored in the house longer period of time.

Observing both figures it can be see how each model performs in different temperature situation given the same input data. Hence, we can conclude that the models fit, thus verifying the control model derived in 2.1 which will be used further in the implementation.



(a) February



(b) July

Figure 2.4: Simulation and control model comparison showing indoor temperature $T_{A,hifi}$ and $T_{A,ctrl}$ in two different weather scenarios with outdoor temperature T_O .

2.2 PV System

In order to take advantage of the sun, one or more solar panels are needed to be put in series or in parallel. A solar panel is composed out of multiple photovoltaic cells connected in series. Such that, a solar cell absorbs some of the light particles falling on it, called photons each of them containing small amounts of energy. Thus, when a photon is absorbed, it releases an electron of solar cell material. Since every part of the solar cell is connected to a cable, a current will flow through it causing the cell to produce electricity that can be used immediately or stored in the battery. In the case when the battery is full and there is no other household consumption the surplus power can be given to the electricity grid or stored as heat. Depending from what material the solar cells are manufactured their efficiency differ. Moreover, the efficiency of the cell is measured in the percentage of irradiance solar energy which is transformed into electric energy.

$$P_{rated} = \eta_{PV} * A_{PV} * I_{rated} \quad (2.25)$$

In most cases, there are some restrictions regarding the total nominal power of a household PV system, to give an example, according to the energy authority in Denmark the total nominal power should not exceed 6 kW [12]. Knowing this, it is mandatory to calculate beforehand the rated power of target PV system. Such that, knowing the rated irradiance value ($I_{rated} = 1kW/m^2$, found in [5]), the efficiency of each PV module η_{PV} and the total area of the system A_{PV} it is possible to compute the rated power P_{rated} of the PV system by using Equation (2.25). To give some examples, in Table 2.1 there are presented different types of installed PV systems and their corresponding peak power. Given the fact that the PV panels are typically overrated a possibility is to install a larger system and when necessary limit the power produced in the inverter.

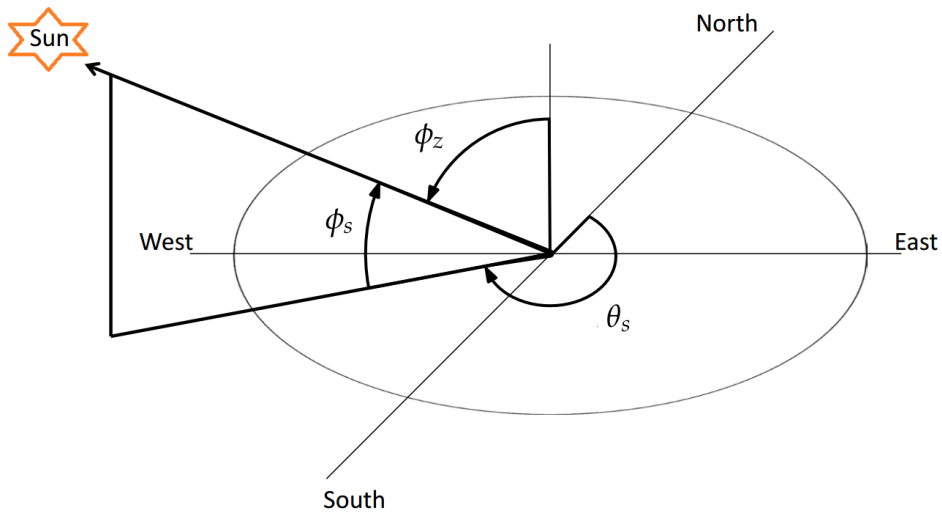
No	$A_{PV} [m^2]$	$\eta_{PV} [\%]$	$P_{peak} [kW]$
1	20	20	4
2	30	20	6
3	40	15	6
4	40	20	8

Table 2.1: Examples of parameters of PV system and total nominal power

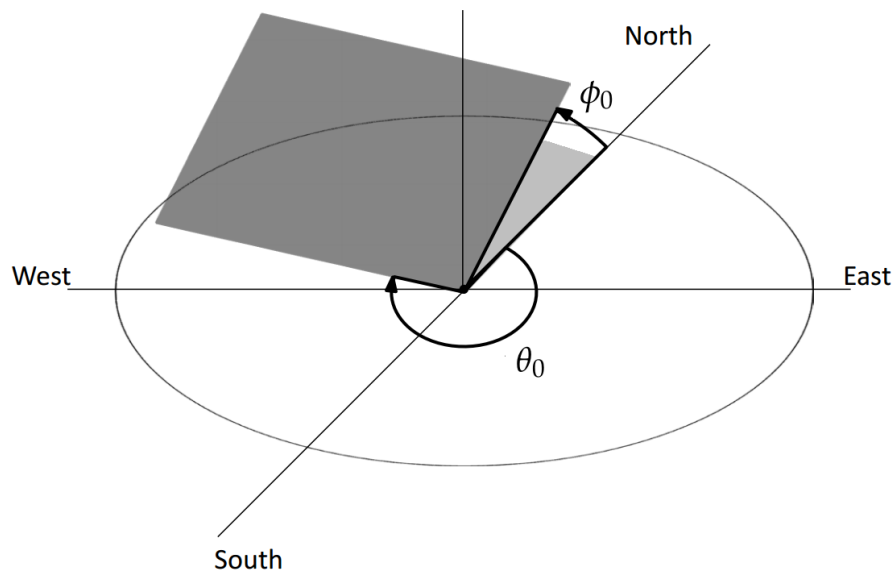
Further, in order to build a near to reality PV generation model the sun incidence angle at each time instance has to be included. Given the fact that Earth is not stationary the sun's angles have to be into account, hence impacting the output power of the PV system. Such that, with respect to the PV array position on the earth the sun azimuth θ_s and altitude ϕ_s angles in Figure 2.5a can be determined based on models found in [13]. Additionally, the zenith angle ϕ_z can be calculated

with Equation (2.26). Both azimuth and zenith angles will be needed forward to determine the sun incidence angle on the PV array.

$$\phi_z(t) = \frac{\pi}{2} - \phi_s(t) \quad (2.26)$$



(a) Sun orientation with azimuth angle, θ_s , altitude angle ϕ_s and zenith angle ϕ_z .



(b) PV array orientation with azimuth angle, θ_0 , and tilt angle ϕ_0 .

Figure 2.5: Sun and PV array orientation.

Furthermore, observing Figure 2.5b, the PV array is fixed on the surface and its orientation is composed out of the azimuth angle θ_0 and tilt angle ϕ_0 . These angles are based on the geometric relationships defined by the array orientation and sun angles.

Given the sun and PV array orientations one can compute the sun incidence angle, α_{sun} , defined as the angle between the beam irradiance and a line normal to the PV array surface. Thus, using Equation (2.27) the incidence angle can be calculated.

$$\alpha_{sun}(t) = \sin \phi_z(t) \cos (\theta_s(t) - \theta_0) \sin \phi_0 + \cos \phi_z(t) \cos \phi_0 \quad (2.27)$$

The output power of the PV system, P_S , depends on the sun incidence angle α_{sun} and direct normal irradiance I_b at time t given by the daily weather forecast as seen in Equation (2.28). Moreover, the parameters of the PV system: area A_{PV} , module efficiency η_{PV} , azimuth θ_0 and tilt ϕ_0 angles are constant.

$$P_S(t) = \eta_{PV} \cdot A_{PV} \cdot I_b(t) \cos \alpha_{sun}(t) \quad (2.28)$$

2.3 Energy Storage

In the case of an “off-grid” house scenario energy storage has to be taken into account. Such that, the power generated by the PV system related in Section 2.2 has to be stored. To give an example, a possible home energy storage based on Lithium-Ion battery modules which supports complete disconnection from the grid supply.

The energy storage dynamics is based on [6] and in Figure 2.6 an example is shown how can it be connected to other components of the system. Hence, the energy stored E_B is expressed in Equation (2.29) by means of the initial battery level $E_B(0)$ and the difference between power from PV generation $P_{B,in}$ and consumption $P_{B,out}$ in time which is denoted by $P_B(t)$. Additionally, the charging and discharging efficiency defined by η in (2.30) are taken into consideration in the model along with the battery drain rate η_d . Moreover, the main limitation of the energy storage is set by the constraint in (2.31), where $E_{B,min}$ and $E_{B,max}$ are the minimum and maximum battery energy levels. In addition, the power ramp limitations on P_B are included in (2.32), where $P_{B,min}$ and $P_{B,max}$ are the minimum and maximum power consumption/injection in the battery.

$$E_B(t) = \eta_d E_B(0) + \int_0^t \eta \underbrace{[P_{B,in}(t) - P_{B,out}(t)]}_{P_B(t)} dt \quad (2.29)$$

$$\eta = \begin{cases} \eta_{in}, & \text{for } P_B(t) \geq 0 \\ \eta_{out}, & \text{for } P_B(t) \leq 0 \end{cases} \quad (2.30)$$

$$E_{B,min} \leq E_B(t) \leq E_{B,max} \quad (2.31)$$

$$P_{B,min} \leq P_B(t) \leq P_{B,max} \quad (2.32)$$

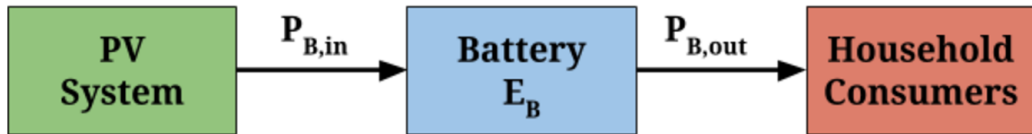


Figure 2.6: Energy storage block diagram usage example.

2.4 Discrete Models

In order to solve the problem in the context of convex optimization in Chapter 3, there is a need to discretize the models present in this chapter. Looking at the block diagram in Figure 2.7 all the GSHS components can be seen while in Table 2.2 the list of variables is presented. Given the fact that there are distinctive components and variables present within the GSHS, an adequate sampling time has to be defined. Hence, the sampling time T_s is considered to be 15 minutes on account of the weather data based on the assumption that there are no drastic changes within this time interval. Also, this period acts as a safeguard measure for the HVAC and backup generator since there should be a limitation between ON/OFF cycles.

Given the sampling time T_s is 15 minutes a day would be divided into 96 time slots k , where the first time slot ($k = 1$) starts at 00:00 and end at 00:15 which is the starting time of second slot ($k = 2$) whilst the last time slot ($k = 96$) in that day will start at 23:45 and end at 00:00. Such that, this can be extended for any number k when multiple day scheduling of the GSHS.

Having the continuous-time house dynamic model obtained in Section 2.1 this should further be discretized. Thus, by employing zero-order hold to the state-space in (2.6) with the sampling time T_s (15 minutes = 0.25 hour), the discrete-time model is obtained in Equation (2.33), where the matrices (A_d, B_d) and vectors (x, u) are the same dimensions as their continuous-time counterparts. The weather data (Q_R, T_O) is provided as inputs to the house model by the simulation tool GridLAB-D [19] at each sample while the control input P_H will be managed by the

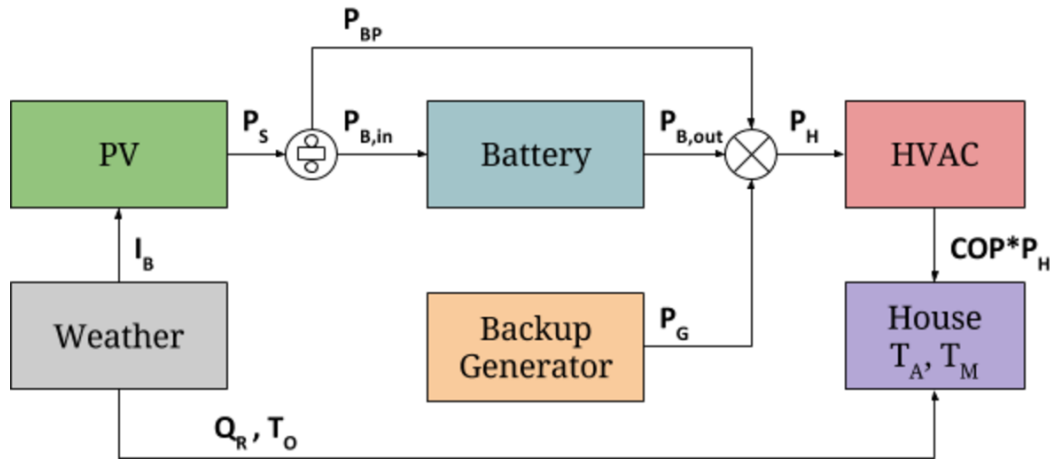


Figure 2.7: GSHS block diagram logic showing the power flows and how the weather impacts the system.

optimization.

$$\begin{aligned} x(k+1) &= A_d x(k) + B_d u(k) \\ y(k) &= C_d x(k) \end{aligned} \quad (2.33)$$

where,

$$\begin{aligned} x(k) &= [T_A(k) \quad T_M(k)]^T \\ u(k) &= [P_H(k) \quad Q_R(k) \quad T_O(k)]^T \\ y(k) &= [T_A(k) \quad T_M(k)]^T \end{aligned}$$

The PV system continuous-time model described in Section 2.2 is given in discrete form in Equation (2.34). Knowing that the PV generation depends on the weather data which consists of the solar irradiance I_b and sun incidence angle α_{sun} which are reduced to the solar irradiance beam I_B as this input will be given directly by the simulation tool GridLAB-D [19] for each sample.

$$P_S(k) = \eta_{PV} \cdot A_{PV} \cdot \underbrace{I_b(k) \cos \alpha_{sun}(k)}_{I_B(k)} \quad (2.34)$$

Regarding the energy storage dynamics presented in 2.3 will have the corresponding discrete form described by Equation (2.35). The intake power $P_{B,in}$ is given in Equation (2.36), where P_{BP} is the power bypassing the battery for HVAC direct usage and P_S is the power generated by the PV system. On the other hand, the output power $P_{B,out}$ is drained for HVAC consumption in the case of inexistent PV generation. In the situation when the battery would empty between time samples, this would be handled by the constraints imposing that enough energy is stored inside it for a whole sampling period.

$$E_B(k+1) = \eta_d E_B(k) + T_s [\eta_{in} P_{B,in}(k) - \eta_{out} P_{B,out}(k)] \quad (2.35)$$

$$P_{B,in}(k) = P_S(k) - P_{BP}(k) \quad (2.36)$$

Last but not least, a backup generator running on fossil fuels with output power P_G is included in (2.37) as a last energy resource in the case of energy shortage when PV generation or energy storage is not available. In the case of a negative power P_G , a zero value will be given by the constraint while having a large positive power value will be limited to an upper bound.

$$P_G(k) = P_H(k) - P_{BP}(k) - P_{B,out}(k) \quad (2.37)$$

Notation	Unit	Description
T_A	[°C]	Temperature of the house air
T_M	[°C]	Temperature of the house mass
T_O	[°C]	Outdoor temperature
P_S	[W]	Power output of PV system
P_G	[W]	Power output of backup generator
P_H	[W]	Power consumption of HVAC system
P_{BP}	[W]	Power bypassing the battery for HVAC consumption
$P_{B,in}$	[W]	Power intake from the PV system
$P_{B,out}$	[W]	Power drained from the battery for HVAC consumption
E_B	[kWh]	Energy stored in the battery
Q_R	[W]	Heat transfer from solar radiation
I_B	[W/m ²]	Solar beam irradiation
A_{PV}	[m ²]	Area of the PV system
η_{PV}	[%]	Efficiency of PV modules
η_d	[%]	Battery drain rate
η_{in}	[%]	Battery charging efficiency
η_{out}	[%]	Battery discharging efficiency
COP	[–]	Coefficient of performance of HVAC
T_s	[s]	Sampling time
k	[–]	Time slot

Table 2.2: List of variables of the GSHS

Chapter 3

Optimization

This chapter deals with solving the optimization problem of the green smart house system (GSHS) presented in Chapter 2 which in this case will be to minimize the backup generator usage and consequently reduce fossil fuels consumption. Such that, in Section 3.1 the objective function will be formulated with the constraints defined in 3.2 and the problem variables given in 3.3. Furthermore, in Section 3.4 the control strategy used for optimization will be presented while in 3.5 the implementation method will be approached.

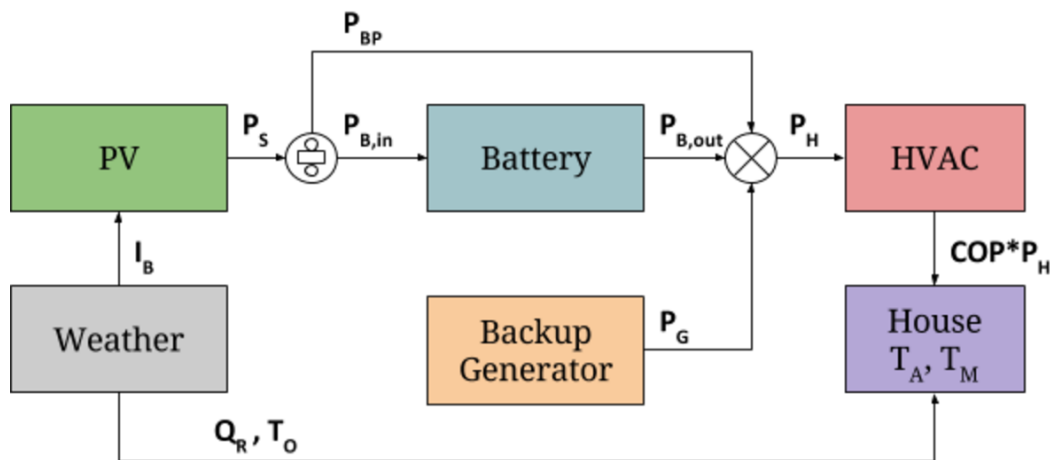


Figure 3.1: GSHS block diagram logic showing the power flows and how the weather impacts the system.

3.1 Objective Function

The scope of this section is to state the problem and construct the objective function that will minimize backup generator usage P_G while keeping the house air temperature T_A to a reference $T_{A,ref}$ for user comfort. First, by looking at the block diagram in Figure 3.1 the following GSHS components can be identified:

- *House* with defined parameters given in Table 3.4 that relate to its construction will be observed at each time step in order to maintain the indoor temperature within an interval. Moreover, the house dynamic model will depend on the weather conditions and heat provided by the HVAC system.
- *HVAC* system will provide heating to the house based on the power intake P_H and *COP* factor. The sources supplying power to the HVAC are as follows: (1) PV generation P_S , (2) battery $P_{B,out}$ and (3) backup generation P_G (each number symbolizes the priority on which source should be used first when it is available).
- *PV* system has specific parameters provided in Table 3.4 and will generate power P_S depending on solar irradiation I_B . The power will be either stored $P_{B,in}$ into the battery or bypassed P_{BP} to the HVAC for immediate use.
- *Battery* that stores the power from the *PV* system for later usage. Moreover, the battery model is characterized by parameters that can be found in Table 3.4.
- *Backup generator* used in the case of insufficient power for the *HVAC* consumption P_H . However, the aim of the optimization is to minimize the generator usage.
- *Weather* data (forecast) that provides the outdoor temperature T_O , solar radiation Q_R and solar irradiance beam I_B used in the *PV* and *House* models to predict future values of generated power P_S and house temperature T_A . Moreover, these predicted values will help on finding optimal values for *HVAC* consumption P_H and *backup generator* output power P_G .

As stated before, the house temperature depends on HVAC heating to keep the temperature within an interval. Such that, an optimization task is to find the optimal values for HVAC power consumption P_H . Moreover, in the case of insufficient power the backup generator needs to be used in order to provide power to the heating system. Thus, there is a need in declaring a multiple objective function $J(\cdot)$ that will satisfy the needs of the GSHS.

As a first and main objective in (3.1) the usage cost of the backup generator P_G has to be minimized, consequently reducing fossil fuels consumption.

$$f_{O1} = \text{minimize } \sum_{k=1}^N P_G(k) \quad (3.1)$$

The second objective in (3.2) deals with the comfort of the household, meaning that a big difference between house air temperature T_A and the predefined reference temperature $T_{A,ref}$ will issue a demand to the HVAC to provide heat.

$$f_{O2} = \text{minimize } \sum_{k=1}^N |T_A(k) - T_{A,ref}(k)| \quad (3.2)$$

The last objective in (3.3) regards minimizing the battery usage $P_{B,out}$ with the idea of giving priority to the use of power generated by the PV system which bypasses the battery P_{BP} for direct HVAC consumption.

$$f_{O3} = \text{minimize } \sum_{k=1}^N P_{B,out}(k) \quad (3.3)$$

Further, by combining all the objectives from Equation (3.1), (3.2) and (3.3), the main objective function $J(\cdot)$ can be built in Equation (3.4). Moreover, in order to match the units difference and to establish which objective is a priority proper weight factors have to be defined for each. Such that, a larger weight on temperature W_T than on backup generator usage W_G and battery W_B provides comfort at the expense of higher energy consumption. Since the aim is to use less fossil fuels, the weight factor W_G should have a higher impact on the objective function in (3.4), followed by the weight on temperature W_T and last being the battery W_B .

$$J(T_A(k), T_{A,ref}(k), P_G(k), P_{B,out}(k), W_T, W_G, W_B) = \sum_{k=1}^N |T_A(k) - T_{A,ref}(k)|W_T + P_G(k)W_G + P_{B,out}(k)W_B \quad (3.4)$$

Finally, the optimization problem is formulated as in (3.5), where the multiple objective function $J(\cdot)$ described in Equation (3.4) is minimized subject to the discrete models found in Section 2.4 and the constraints that are presented in Section 3.2. The purpose is to find the optimal values for the decision variables found in Table 3.2 that will minimize the function $J(\cdot)$.

$$\begin{aligned} &\text{minimize } J(T_A(k), T_{A,ref}(k), P_G(k), P_{B,out}(k), W_T, W_G, W_B) && (3.5) \\ &\text{subject to (2.33) – (2.35)} \\ &\quad (3.6) – (3.14) \end{aligned}$$

3.2 Constraints

This section continues with establishing the constraints of the optimization problem at hand. To begin with the constraint on the backup generator as given in (3.6), where P_{BP} is the power bypassing the battery and depends on PV generation P_S and should be used as a first resource, $P_{B,out}$ is the power drained from the battery and P_H represents the power consumption of the heating system at time slot k . Furthermore, the limitation on backup power generation P_G is dealt by (3.7), where $P_{G,max}$ is the maximum output power of the generator.

$$P_H(k) = P_{BP}(k) + P_{B,out}(k) + P_G(k) \quad (3.6)$$

$$0 \leq P_G(k) \leq P_{G,max} \quad (3.7)$$

Considering the discrete house model in Equation (2.33), the constraint on mass temperature T_M can be defined in (3.8) with the comfort interval set by the minimum $T_{M,min}$ and maximum $T_{M,max}$ bounds. The reason why there is no constraint on the air temperature T_A is that feasibility problems may occur, since it is directly in the objective function (3.4).

$$T_{M,min} \leq T_M(k) \leq T_{M,max} \quad (3.8)$$

HVAC limitation constraint on how much power P_H it can consume is given in (3.9), where $P_{H,max}$ is the maximum power that can be provided to the system.

$$0 \leq P_H(k) \leq P_{H,max} \quad (3.9)$$

Regarding the energy storage, an important constraint has to be defined in (3.10) for the power. Additionally, the battery level limitation is given in (3.11) by the lower $E_{B,min}$ and upper $E_{B,max}$ bounds of energy level. Moreover, the limit on power injection $P_{B,in}$ is managed by constraint (3.11) while the inequality (3.12) deals with bounding the output power $P_{B,out}$ of the battery, where $P_{Bi,max}$ and $P_{Bo,max}$ are the upper bounds for injection and consumption respectively. Last but not least, the constraint on the power bypassing the battery P_{BP} is limited to the total generation P_S provided by the PV system.

$$P_S(k) = P_{B,in}(k) + P_{BP}(k) \quad (3.10)$$

$$E_{B,min} \leq E_B(k) \leq E_{B,max} \quad (3.11)$$

$$0 \leq P_{B,in}(k) \leq P_{Bi,max} \quad (3.12)$$

$$0 \leq P_{B,out}(k) \leq P_{Bo,max} \quad (3.13)$$

$$0 \leq P_{BP}(k) \leq P_S(k) \quad (3.14)$$

3.3 Problem Variables

In this section a classification of the problem variables will be done before a thorough implementation will take place. First, the variables that represent the dynamics of each model presented in Section 2.4 can be seen in Table 3.1.

Variable	Unit	Description
T_A	[°C]	Temperature of the house air
T_M	[°C]	Temperature of the house mass
P_S	[W]	Power output of PV system
E_B	[kWh]	Energy stored in the battery

Table 3.1: List of model variables

Secondly, the list with all the decision variables is given in Table 3.2. These variables may change their values over the runtime of the optimization to solve the problem in an optimal way.

Variable	Unit	Description
P_H	[W]	Power consumption of HVAC system
P_G	[W]	Power output of backup generator
P_{BP}	[W]	Power bypassing the battery for HVAC consumption
$P_{B,in}$	[W]	Power intake from the PV system
$P_{B,out}$	[W]	Power drained from the battery for HVAC consumption

Table 3.2: List of decision variables

Furthermore, expressions and constraints rely on other data to perform the calculations to find the optimal values for the decision variables. Particularly, the list of data inputs is presented in Table 3.3, where this data is provided through the use of the simulation tool GridLAB-D [19].

Data	Unit	Description
T_O	[°C]	Outdoor temperature
Q_R	[W]	Heat transfer from solar radiation
I_B	[W/m ²]	Solar beam irradiation

Table 3.3: List of data inputs

Last but not least, the parameters that define all the GSHS components and simulation specification are described in Table 3.4. The parameters regarding each component relate to the construction or characteristic of the house, battery, HVAC or PV system, whilst the simulation parameters describe how the system should perform and within which boundaries. Moreover, each parameter can be modified

and tuned in order to create specific, close to reality, scenarios. To be noted that, the list of variables can be extended by improving existing components or adding new ones to the GSHS, thus making the problem more complex and realistic.

Parameter	Unit	Description
$T_{A,ref}$	[°C]	House reference temperature
$T_{A,min}$	[°C]	House minimum allowed temperature
$T_{A,max}$	[°C]	House maximum allowed temperature
$P_{H,max}$	[W]	HVAC maximum power consumption
$P_{G,max}$	[W]	Backup generator maximum power output
$P_{Bi,max}$	[W]	Battery maximum power injection
$P_{Bo,max}$	[W]	Battery maximum power output
$E_{B,min}$	[kWh]	Battery minimum level
$E_{B,max}$	[kWh]	Battery maximum level
E_{B0}	[kWh]	Battery initial level
W_T	[–]	Weight factor on temperature temperature
W_G	[–]	Weight factor on backup power generation
W_B	[–]	Weight factor on battery usage
U_M	[W/°C]	House mass surface conductance
U_A	[W/°C]	House envelope conductance
C_M	[J/°C]	House thermal mass capacitance
C_A	[J/°C]	House air thermal capacitance
A_{PV}	[m ²]	Area of the PV system
η_{PV}	[%]	Efficiency of PV modules
η_d	[%]	Battery drain rate
η_{in}	[%]	Battery charging efficiency
η_{out}	[%]	Battery discharging efficiency
COP	[–]	Coefficient of performance of HVAC
T_s	[s]	Sampling time
k	[–]	Sampling step
N	[–]	Prediction horizon

Table 3.4: List of system parameters

3.4 Model Predictive Control

In order to handle the optimization problem stated in Section 3.1 this study will look into the framework of predictive control, particularly Model Predictive Control (MPC). The main reason for choosing this is that MPC is the control technology which can handle multivariable control problems, deal routinely with diverse equipment and safety constraints [21]. Furthermore, it is necessary to point out the essential features of the predictive control strategy such as:

1. *Internal model* capable of simulating and predicting the plant behaviour faster than real time.
2. *Receding horizon idea* in which the prediction horizon remains the same length, whilst moving along by one sampling interval at each step.
3. *Computation of future control inputs* which optimizes the predicted plant behaviour.

Thus, having the predicted behaviour of the plant depending on the assumed control inputs, over a future prediction horizon, it is possible to choose the input that would result in the best predicted behaviour. To be noted that, each future control input is given depending on the conditions at the current time frame. Moreover, in the case of having several inputs that would result in the same behaviour, it is preferable (in the case at hand) to choose the input that requires the least amount of energy to be spent.

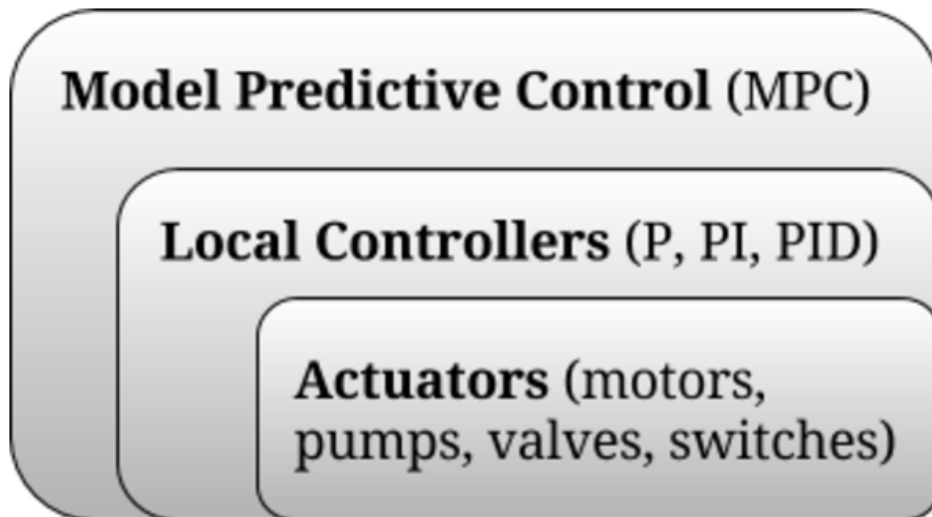


Figure 3.2: Control hierarchy of current setup.

Control hierarchy

On another note, there is a need to discuss the different control layers which present within the GSHS. Such that, by taking a look at the control hierarchy of the current setup as depicted in Figure 3.2, it can be observed that at the bottom level there are, depending on each component, control loops associated with individual actuators, such as motors, pumps, valves and switches. Going a layer upwards, the traditional controllers: proportional (P), proportional-integral (PI) and proportional-integral-derivative (PID) can be found individually controlling pressure, temperatures, voltages, currents on each system respectively. On top of these, the MPC layer is comparable to a bridge between the different components present inside the GSHS. Moreover, this upper layer deals with all the conditions which cannot be fulfilled by the elementary one control loop paradigm.

MPC advantages

To make a comparison with the classical PID-controller based control solution, one advantage of MPC is that it integrates useful future information in taking control decisions, for example incorporate forecast weather data as outdoor temperature, solar radiation and other predicted disturbances in the optimization procedure. Another advantage of using MPC in the case at hand is that it allows definition of system constraints, for example defining house temperature intervals or finite amount of heating power of HVAC system. As a last advantage, MPC can find the optimal control actions to fulfill the goals of the system which can be using less energy, or less fossil fuels, or keeping the temperature to a reference, or their combination. On the other hand, a disadvantage of using MPC is related to the computing power necessities. For example, in the case of a complex problem with a high number of variables, depending on the processing capabilities available, the time required to compute the optimal inputs may vary from a few seconds to several hours. Given the recent advancements in technology, at this moment of the writing, computing power required to run MPC has become less troublesome.

Problem assumptions

First of all, we shall assume that the internal model that will be used further on is linear, whilst the predictions will be made over constant prediction horizon. Another important assumption that has to be made is in regards to the previous air T_A and mass T_M temperatures required for each new iteration. Such that, further we shall assume that these temperatures are either measured by a sensor or estimated by an observer.

MPC problem

Given the background and advantages posed earlier in this section, the problem in (3.5) is reformulated in the context of MPC. Such that, the objective function in Equation (3.15) is minimized subject to the discrete models found in Section 2.4 and the constraints that are presented in Section 3.2.

$$\text{minimize } \sum_{i=0}^{N-1} |T_A(k+i) - T_{A,ref}(k+i)|W_T + P_G(k+i)W_G + P_{B,out}(k+i)W_B \quad (3.15)$$

subject to (2.33) – (2.35)

(3.6) – (3.14)

where,

- N is the prediction horizon, chosen to compute the next control sequence;
- $k = 1, 2, \dots, 96$ is the current sampling step that relates to a sampling time of 15 minutes, which means that a day would be divided into 96 time slots k , where the first time slot ($k = 1$) starts at 00:00 and end at 00:15 which is the starting time of second slot ($k = 2$) whilst the last time slot ($k = 96$) in that day will start at 23:45 and end at 00:00;
- $i = 0, 1, \dots, N - 1$ is the iteration step;
- $T_A(k+i)$ is the air temperature predicted at step $k+i$, by applying the inputs to the house model in (2.33) starting from current temperature $T_A(k)$;
- $T_{A,ref}(k+i)$ is the house reference temperature that has to be taken into account at time step $k+i$;
- $P_G(k+i)$ is the predicted optimal value for backup generation at time step $k+i$ which needs to be fulfilled in the absence of other power sources;
- $P_{B,out}(k+i)$ is the predicted optimal value for battery usage at time step $k+i$, which provides power to the heating system;
- W_T temperature weight, W_G backup generator usage weight, W_B battery usage weight factors used to balance the GSHS requirements, chosen as described in Section 3.1 and later on in the simulation.

The goal of the MPC problem described above is to find the optimal values for the decision variables found in Table 3.2 over a prediction horizon N , by iterating from the current state k of the system until the end of the horizon, namely at time $k+N$. Thus, knowing the requirements of the MPC problem, further we shall look into how to implement it.

3.5 Convex Optimization

In this section the theoretical background of convex optimization is presented which comes as a prerequisite in order to implementing the MPC problem described in Section 3.4.

To be noted that there are several way of implementing MPC, an example is to formulate the problem as a *quadratic (QP) or linear (LP) program* as described in [21] and solving them using standard Matlab function such as *quadprog()* or *linprog()*. However, formulating the problem as a QP or LP is often possible, but in this case it requires reformulating the actual optimization problem, by adding other variables and constraints in order to get it into QP or LP form. These methods would demand extra preparatory work, for example expanding the control system in order to cover the whole prediction horizon, before using the Matlab functions aforementioned. Moreover, this implies an augmented implementation, which can be prone to mistakes and eventually more time consuming.

Considering the problem formulated along this chapter it has been decided that this study will focus on convex optimization by using Matlab and a plugin called CVX [14]. In particular, this method has been chosen since it respects all the requirements of the optimization problem at hand such as handling multi objectives, constraints and finding the decision variables needed as control inputs to the whole GSHS.

As a first step, formulating the problem in 3.4 as a convex optimization problem is atmost important in order to solve it efficiently. Such that, by observing Equation (3.16) the general form of the convex optimization problem is presented, as found in [10].

$$\begin{aligned}
 & \text{minimize } f_0(x) \\
 & \text{subject to } f_i(x) \leq b_i, \quad i = 1, \dots, m \\
 & \quad \quad \quad h_j(x) = c_j, \quad j = 1, \dots, p
 \end{aligned} \tag{3.16}$$

where,

- $x = x_1, \dots, x_n$ is the *optimization problem variable*;
- $f_0 : \mathbb{R}^n \rightarrow \mathbb{R}$ is the *objective function*;
- $f_i : \mathbb{R}^n \rightarrow \mathbb{R}$ with $i = 1, \dots, m$, are the *inequality constraint functions*;
- b_1, \dots, b_m are the *constraints boundaries for inequalities*;
- $h_j : \mathbb{R}^n \rightarrow \mathbb{R}$ with $j = 1, \dots, p$, are the *equality constraint functions*;
- c_1, \dots, c_p are the *constraints boundaries for equalities*;

- $x^* = x_1^*, \dots, x_n^*$ is the *solution of the problem*, if it gives the lowest objective function of all vectors which satisfy the following constraints $\forall z$:

$$\begin{aligned} f_0(z) &\geq f_0(x^*) \\ f_1(z) &\leq b_1, \dots, f_m(z) \leq b_m \\ h_1(z) &= c_1, \dots, h_p(z) = c_p \end{aligned}$$

Moreover, in order for the optimization problem to be convex this implies that the objective and constraint functions are convex, that is satisfying the inequality given in Equation (3.17) for all $x, y \in \mathbb{R}^n$ and all $\alpha, \beta \in \mathbb{R}$, knowing that $\alpha + \beta = 1$ with $\alpha \geq 0$ and $\beta \geq 0$. This inequality would imply that the line segment between $(x, f_i(x))$ and $(y, f_i(y))$ lies above the graph of the function f_i as pictured in Figure 3.3.

$$f_i(\alpha x + \beta y) \leq \alpha f_i(x) + \beta f_i(y) \quad (3.17)$$

On the other hand, in the case where the constraint functions are equalities they would obey Equation (3.18) for all $x, y \in \mathbb{R}^n$ and all $\alpha, \beta \in \mathbb{R}$, knowing that $\alpha + \beta = 1$. For affine functions as in (3.18) it is already implied that they are convex if the equality holds. Controversely, it can be said that any function that is convex is also affine.

$$h_i(\alpha x + \beta y) = \alpha h_i(x) + \beta h_i(y) \quad (3.18)$$



Figure 3.3: Graph of a convex function, where the line segment between any two points on the graph, for example the chord from x and y , stands above the graph.

Furthermore, the domain \mathcal{D} of the optimization problem is given by Equation (3.19), representing the set of points for which the objective function and all constraint functions are defined. The problem is said to be *feasible* if there exists at least one feasible point $x \in \mathcal{D}$ which satisfy the constraints in Equation (3.16), and *infeasible* otherwise.

$$\mathcal{D} = \bigcap_{i=0}^m \mathbf{dom} f_i \cap \bigcap_{j=1}^p \mathbf{dom} h_j \quad (3.19)$$

CVX is a modeling framework that allows convex programs to be specified in a mathematical form. However, the use of CVX requires that one must obey the rules governed by disciplined convex programming (DCP). Thus, to give an example a set of rules of DCP will be given as found in [20], followed by an analysis of the optimization problem presented in this chapter:

- Problem type, a valid DCP can be:
 - “T1 a minimization: a convex objective and zero or more convex constraints”;
 - “T2 a maximization: a concave objective and zero or more convex constraints”;
- Constraints can be:
 - “T4 an equality constraint with affine left- and right-hand expressions”;
affine = affine
 - “T5 a less than ($<$, \leq) inequality, with a convex left-hand expression and a concave right-hand expression”;
convex \leq concave or convex $<$ concave
 - “T6 a greater than ($>$, \geq) inequality, with a concave left-hand expression and a convex right-hand expression”;
concave \geq convex or concave $>$ convex
- Product-free rules:
 1. “The sum of two or more convex (concave, affine) expressions is convex (concave, affine)”;
 2. “The product of a convex (concave) expression and a nonnegative constant expression is convex (concave)”;
 3. “The product of a convex (concave) expression and a nonpositive constant expression, or the simple negation of the former, is concave (convex)”;
 4. “The product of an affine expression and any constant is affine”.

The optimization problem in (3.15) is defined as a minimization $T1$ and further investigation regarding the convexity of the objective function in (3.20) is necessary.

$$\sum_{k=1}^N |T_A(k) - T_{A,ref}(k)|W_T + P_G(k)W_G + P_{B,out}(k)W_B \quad (3.20)$$

- $|T_A(k) - T_{A,ref}(k)|$ is defined as an absolute value function and as detailed in [10] this function is convex.
- $P_G(k)$ is described by the affine function in (3.6) and convex constraint in (3.7), meaning that $P_G(k)$ is convex.
- $P_{B,out}(k)$ is described by the affine function in (3.6) and convex constraint in (3.13), meaning that $P_{B,out}(k)$ is convex.

Furthermore, given that the weight factors (W_T, W_G, W_B) are assumed to be non-negative constants all the objectives obey product-free rule (2) and since they are convex, following rule (1) it can be stated that their sum in (3.20) will be also convex.

Regarding the constraints in Section 3.2, one may observe both convex and affine expressions along the section. Given as reference the rules in $T4$ and $T5$, it can be said and verified that the constraints obey the rules of DCP.

Provided that the current problem is formulated as a convex optimization problem, further implementation of MPC can be pursued using CVX and Matlab. Hence, by the respecting the rules of DCP [20] we can define the objective 3.1, constraints 3.2 and variables 3.3 using CVX tool.

For a smoother understading of the whole optimization problem one can look at the block diagram illustrated in Figure 3.4. This shows how the GSHS provides the current state of the system (of each component) to the MPC block which integrates the weather forecast (Q'_R, T'_O, I'_B) in order to provide the optimal values for the decision variables found in Table 3.2.

Along this section it has been shown that the MPC problem stated in Section 3.4 fits in the context of convex optimization, thus enabling to further pursue a practical implementation using CVX and Matlab [14] that can be found in Appendix A, whilst the simulation results are presented in Chapter 4.

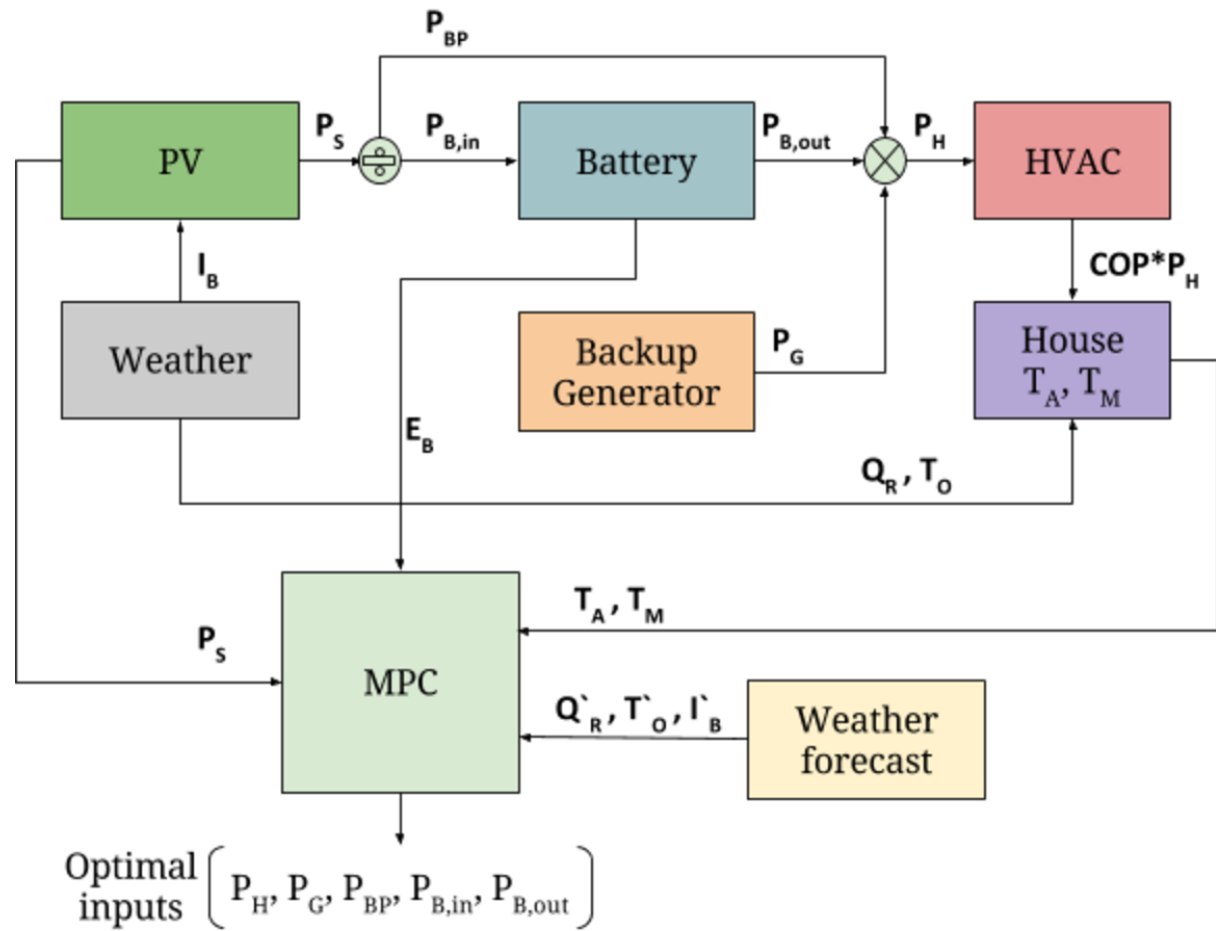


Figure 3.4: Block diagram of GSHS connected with the MPC solver which provides the optimal control inputs based on current state of the system and weather forecast, where the variables found in Section 3.3.

Chapter 4

Simulation

Inside this chapter a series of simulations will be performed regarding the optimization problem found in Equation (4.1), explained along Chapter 3, followed by a discussion based on the results. At first, a preliminary example is shown in Section 4.1 using only the backup generator to exemplify how much power needs to be generated, such that the indoor temperature stays near the reference in a winter scenario. Next, in Section 4.2, an extension is made by integrating the PV system generation and battery energy storage to the GSHS in order to observe the impact on energy generation. Last but not least, a comparison between two different scenarios is provided in Section 4.3 in pursuance of lowering fossil fuel usage.

$$\begin{aligned} & \text{minimize} \quad \sum_{i=0}^{N-1} |T_A(k+i) - T_{A,ref}(k+i)|W_T + P_C(k+i)W_G + P_{B,out}(k+i)W_B \\ & \text{subject to} \quad (2.33) - (2.35) \\ & \quad \quad \quad (3.6) - (3.14) \end{aligned} \tag{4.1}$$

Regarding the implementation, found in Appendix A, this was done in Matlab by making use of the CVX plug-in [14]. The parameters used across all simulations may be observed in Table 4.1, with the mention that the asterisk (*) means that the value may vary depending on the scenario. Moreover, the weight factors in (4.1) are

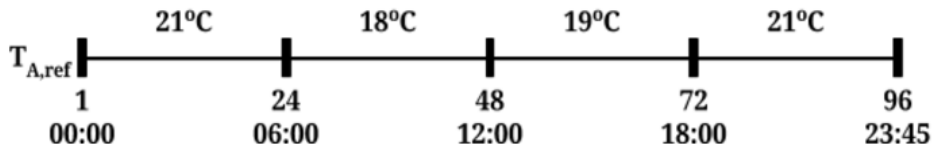


Figure 4.1: House reference temperatures chosen during a day for each 6 hour interval.

chosen taking into account the difference in measurement units, since W_T weighs temperature, whilst W_G and W_B weighs power. Such that, their values are chosen in the idea to keep the house temperature T_A to the reference $T_{A,ref}$ which is set for each time interval, as illustrated in Figure 4.1. The reason for choosing these intervals is that in many cases between the interval 18:00 to 06:00 the inhabitants are in their house, thus the need to choose a temperature near 21 °C. On the other hand, between the interval 06:00 to 18:00 the occupants are most likely to be away, hence lower temperatures of 18-19 °C may be applied for reducing consumption. In regards to the weather data, this is provided by GridLAB-D climate module [17] and it is specific to the climate in the state of Colorado, USA. Moreover, all the simulations are made taking into consideration winter temperatures, hence the scope of this study is limited to provide heating to an usual household.

Parameter	Value	Unit	Description
N	20	[–]	Prediction horizon
$T_{A,min}$	15	[°C]	House minimum allowed air temperature
$T_{A,max}$	24	[°C]	House maximum allowed air temperature
$T_{M,min}$	15	[°C]	House minimum allowed mass temperature
$T_{M,max}$	24	[°C]	House maximum allowed mass temperature
$P_{H,max}$	3	[kW]	HVAC maximum power consumption
$P_{G,max}$	8	[kW]	Backup generator maximum power output
$P_{Bi,max}$	3	[kW]	Battery maximum power injection
$P_{Bo,max}$	5	[kW]	Battery maximum power output
$E_{B,min}$	2	[kWh]	Battery minimum level
$E_{B,max}$	20	[kWh]	Battery maximum level
W_T	*0.7	[–]	Weight factor on temperature temperature
W_G	*0.002	[–]	Weight factor on backup power generation
W_B	*0.001	[–]	Weight factor on battery usage
U_M	9889	[W/°C]	House mass surface conductance
U_A	566	[W/°C]	House envelope conductance
C_M	9286	[kJ/°C]	House thermal mass capacitance
C_A	2290	[kJ/°C]	House air thermal capacitance
A_{PV}	45	[m ²]	Area of the PV system
η_{PV}	20	[%]	Efficiency of PV modules
η_d	99	[%]	Battery drain rate
η_{in}	99	[%]	Battery charging efficiency
η_{out}	101	[%]	Battery discharging efficiency
COP	3.5	[–]	Coefficient of performance of HVAC

Table 4.1: List of GSHS parameters values used throughout the simulations

4.1 Preliminary Example

This preliminary example is meant to provide some insight on the case when only the backup generator is used as a source of power in order to see how important renewable energies are in an "off-grid" situation. Such that, across this scenario simulation the power generated by the PV system P_S and energy storage E_B will be considered zero, as if they are absent.

Given the assumptions made previously at the beginning of this chapter, the preliminary example will run as a MPC problem (4.1), defined in Section (3.4). Moreover, the integration of weather forecast, composed of solar radiation Q_R and outdoor temperature T_O is made over a prediction horizon N of 5 hours, equivalent to 20 samples ahead prediction. Such that, using this weather forecast the predictive controller keeps the house temperature $T_{A,c}$ near the reference $T_{A,ref}$ shown in Figure 4.1. This can be observed in Figure 4.2, where both the house temperature in normal conditions $T_{A,n}$ (without heating) and controlled $T_{A,c}$ start from the same point of 18 °C, but drift apart from each other since $T_{A,c}$ is provided heat from the HVAC system. Moreover, both temperatures are affected by the weather represented by the outdoor temperature T_O and the solar radiation Q_R (scaled in kW, such that it can be observed on the same plot). This in particular can be observed clearly on $T_{A,n}$, where the solar radiation Q_R keeps the house temperature

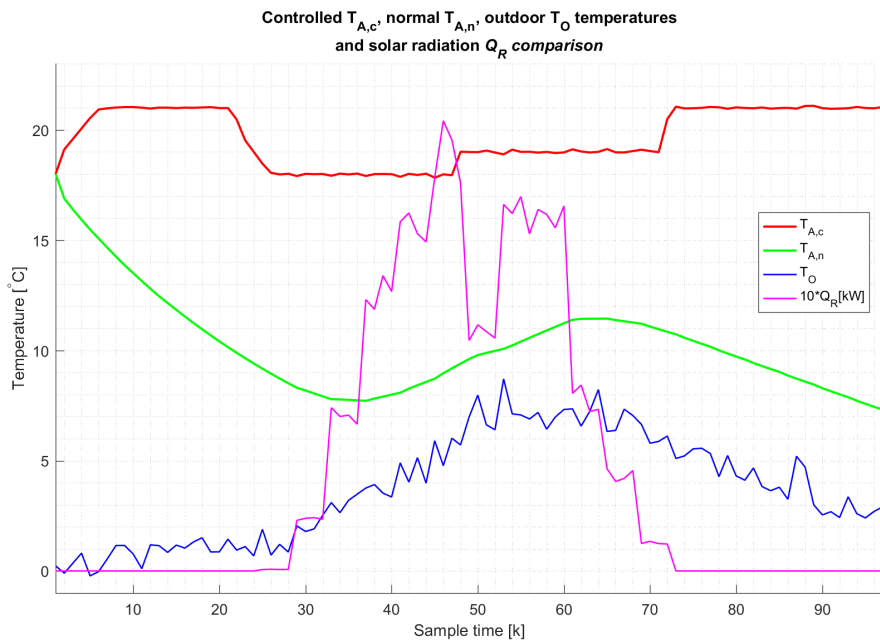


Figure 4.2: Preliminary example: House controlled temperature $T_{A,c}$ with house temperature in normal conditions $T_{A,n}$, outdoor temperature T_O and solar radiation Q_R .

above the ambient temperature T_O with approximately 4-5 °C, from sampling step 40 onwards.

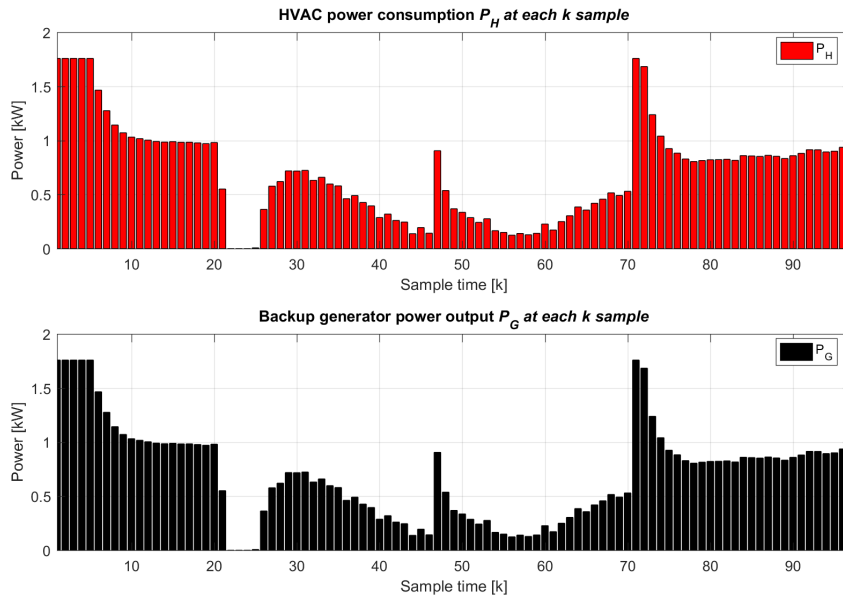
Furthermore, in the case of $T_{A,c}$ the predictive controller is raising the temperature by demanding more heat from the HVAC, whilst $T_{A,n}$ goes down due to the influence of the outdoor temperature T_O . Additionally, a good sign that the MPC is working properly is given by the fact that $T_{A,c}$ firmly follows the reference temperature $T_{A,ref}$ for each interval of the day.

A remark can be made on the sudden fall of Q_R in the middle of the day, samples 47 to 51, due to the cloud coverage during that interval. Even though the impact of the fall is not seen clearly on $T_{A,n}$ this can be observed on the power of the HVAC in Figure 4.3a, where the consumption is greater for samples 47 to 49 than the previous ones in order to compensate for the decrease of solar radiation.

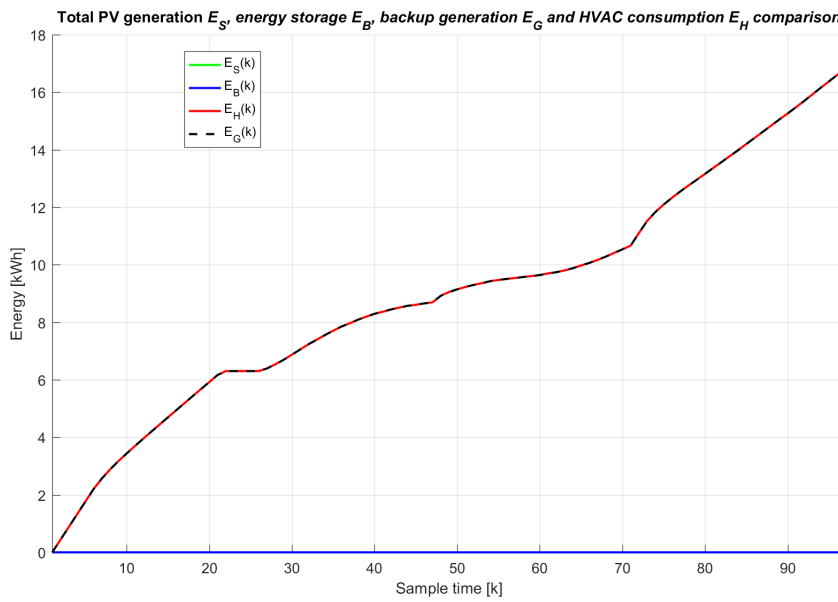
Regarding the power performance of the HVAC, depicted in Figure 4.3a, it can be said that for the first samples the high consumption is matched with the increase in temperature in 4.2. Also, the same is applicable starting from sample 73, where the reference temperature $T_{A,ref}$ changes to 21 °C by means of providing comfort to the inhabitants. On the other hand, the change of the reference to 18 °C, beginning from sample 22 and ending at 25, provides the HVAC with a 'resting time' (OFF mode), hence the zero consumption in that interval seen in 4.3a.

As stated in the beginning of this section, this scenario has been built to take into account only the backup generator as power source and give a sense on how much fossil fuels would be used, by associating this with the power generated P_G . As expected, for this scenario the power consumption of the HVAC P_H is equivalent to the backup generation P_G , as it can be observed in both Figure 4.3a and 4.3b. Also, this serves as an additional confirmation that the implementation is satisfactory for further investigation.

As a last remark, provided the energy profile in Figure 4.3b it can be concluded that the backup generation needed to keep the heating system running for a whole day in the cold season is fairly alarming, totalling 17 kWh. Thus, it is important to investigate further how to exchange some of the backup generation with renewable energies and pursue on to optimizing this process.



(a) Power flows of backup generator P_G and HVAC power consumption P_H at each sample k .



(b) Energy profiles of backup generation E_G and HVAC consumption E_H .

Figure 4.3: Preliminary example: Power and energy performances, excluding PV generation E_S and storage E_B .

4.2 Battery Example

This scenario is built in order to observe the impact on the system when PV generation and energy storage is taken into account. Considering the list of parameters provided in Table 4.1, this example will start with half the energy stored in the battery (10 kWh) and discussed further on the energy performance. Moreover, the reference temperatures considered in the simulations are the same as in Figure 4.1.

Regarding the *weight factors* in the optimization problem (4.1), these are chosen in order to prioritize the needs of the system: **(1)** minimize backup generation W_G , **(2)** keep temperature to reference W_T and **(3)** save battery storage W_B . To give an example, without taking into account the difference regarding the measurements units of each objective, the relation between the weight factors is given as follows: $W_B < W_T < W_G$.

At first, by examining Figure 4.4 one can verify if the constraint in (3.10) is fulfilled. This shows, more or less, how the battery is charged $P_{B,in}$ or/and how much power bypasses P_{BP} for direct consumption, adding up to the solar generation P_S . Moreover, the fluctuations seen on the PV power generation P_S are due to the variations in solar radiation, as pictured in Figure 4.7a. This verifies that the implementation is working within its boundaries, providing a realistic approach to the problem at hand.

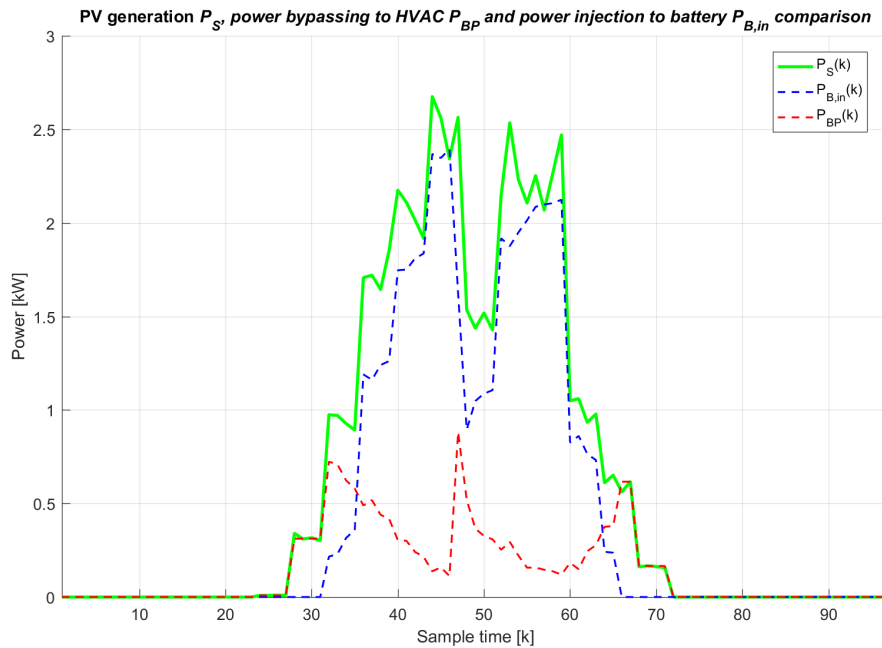


Figure 4.4: Battery example: PV generation P_S splitting the power to bypass P_{BP} to HVAC and power injection to battery $P_{B,in}$.

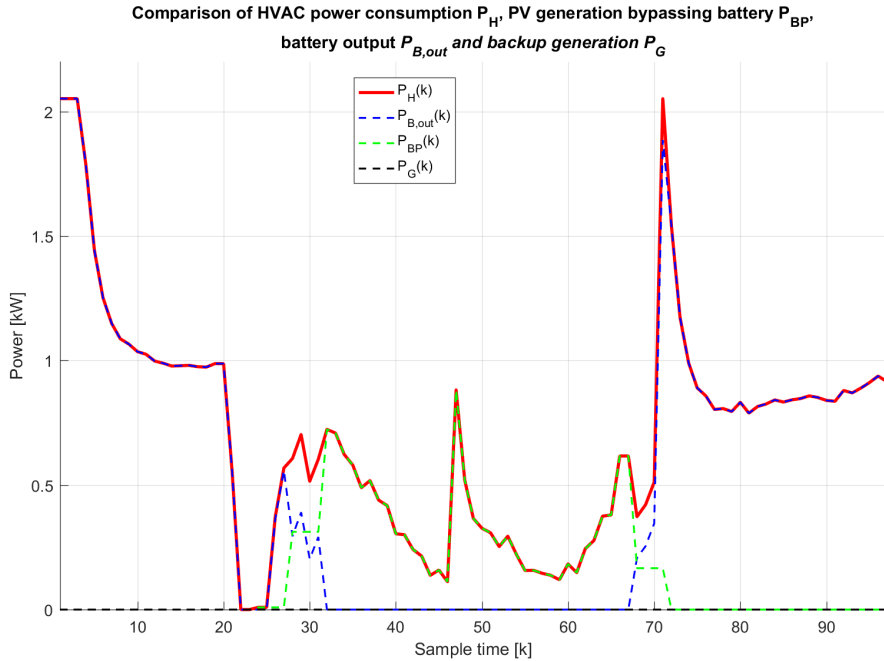


Figure 4.5: Battery example: HVAC power consumption P_H depending on bypass power P_{BP} , power drained from battery $P_{B,out}$ and generated power P_G .

Further on, Figure 4.5 shows all the power sources provided for HVAC consumption P_H . Also, given that from the start the battery output $P_{B,out}$ follows P_H and later on the HVAC load is handled by the PV generation P_{BP} , one can check easily that constraint (3.6) is met. Moreover, it is important to observe if the controller is prioritizing consumption based on PV generation over the other power sources. Such that, it can be seen that as soon as PV generation P_S is available, starting from sample 25, it will immediately bypass the battery P_{BP} and provide power to the heating system P_H . Shortly after sample 32, the consumption switches to use only solar power until sample 68 (equivalent to hour 17:00, sunset).

In order to get an overview of the total energy generated (E_G and E_S), stored E_B and consumed E_H , one may look in Figure 4.6. In the beginning of this section it was stated that the initial battery level is half (10 kWh) of its maximum capacity, this can be verified by looking at the starting point of the energy storage E_B . Also, it can be seen how the energy storage E_B is drained, whilst the HVAC energy consumption E_H increases. Later on, around sample 35, the battery begins to accumulate as a result of PV generation E_S increase. Further, it can be observed that there is no backup generation E_G at all involved, meaning that this would somewhat solve the problem of fossil fuels usage. However, in the problem at hand the other household consumers (e.g. water heater, washing machine, dishwasher)

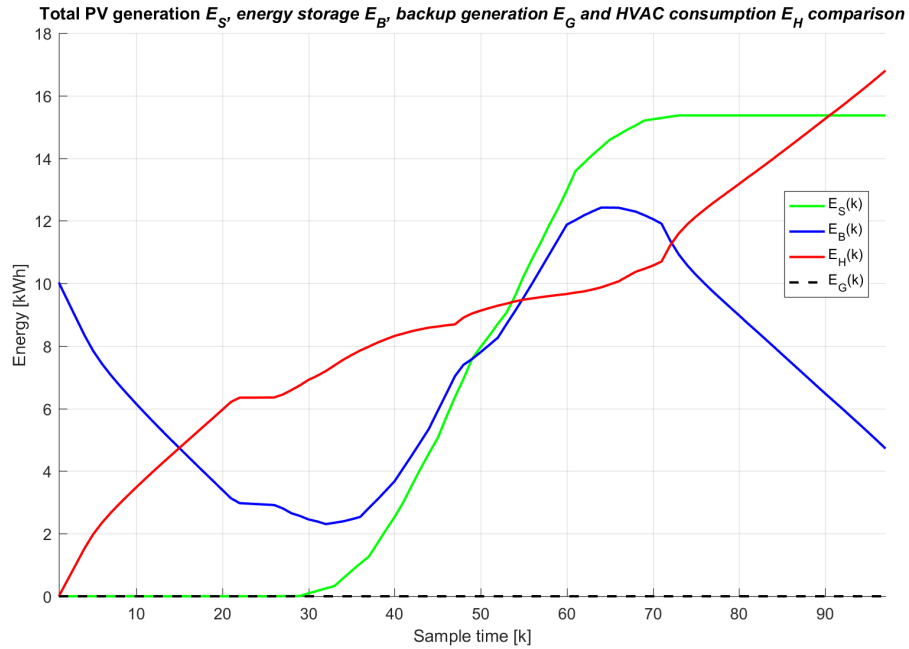
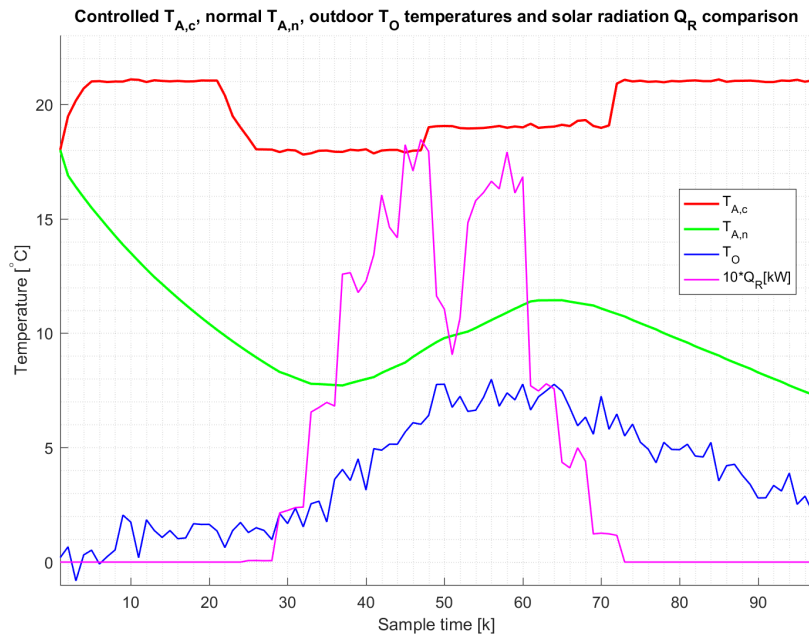


Figure 4.6: Battery example: Energy profile of PV generation E_S , storage E_B , backup generation E_G and HVAC consumption E_H .

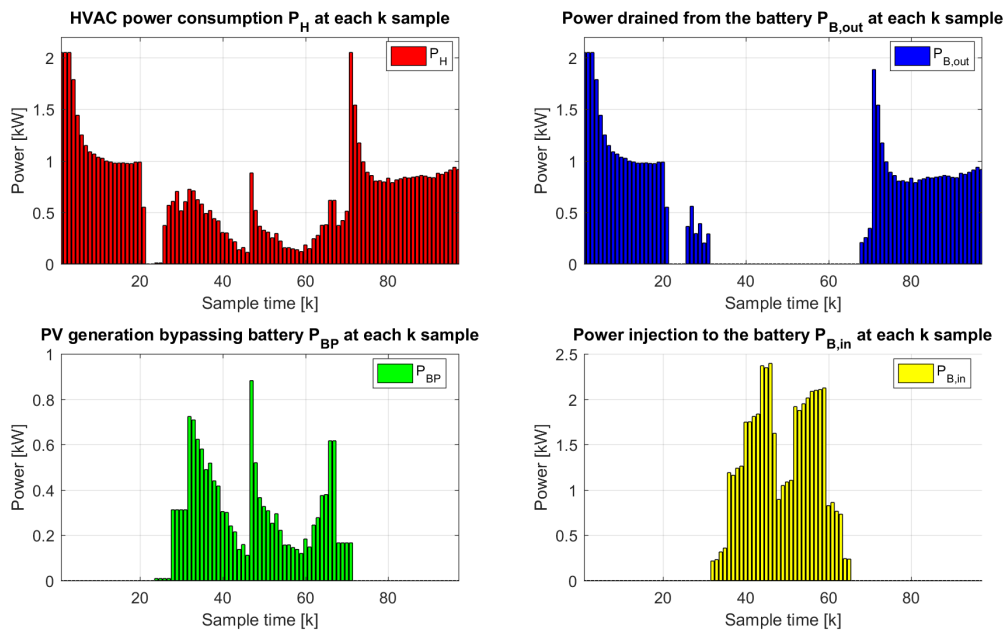
and the inhabitants disturbances are not taken into consideration. Nonetheless, it is a good starting point using only the HVAC system for now since it is the biggest and most important consumer of a household.

Moving on to the controller performance, following temperature $T_{A,c}$ in Figure 4.7a, it can be seen that the HVAC follows through and provides the heat necessary to keep the temperature to the reference $T_{A,ref}$. However, this comes with a cost in power consumption P_H , depicted in Figure 4.7b, starting from the first sample the controller enforces the HVAC to provide an indoor temperature of 21 °C. Hence, this is shown in the HVAC consumption, top left of 4.7b, where within the first 5 samples more power is required, starting from 2 kW and decreasing onwards. Moreover, when the reference lowers to 18 °C (k=22) the heating system takes a break (no consumption) until the house temperature reaches that reference (k=25). Additionally, to confirm that the battery is not charging $P_{B,in}$ and discharging $P_{B,out}$ at the same time one may look on the right side plots of Figure 4.7b.

Based on this scenario we can conclude that the MPC had a good performance with respect to the demands of the system. Moreover, with the assumed half energy storage on a winter day no backup generation was used, but the simulation did not account for other household consumers. Additionally, this example shows how important energy storage and renewable energies are in an "off-grid" scenario.



(a) House controlled temperature $T_{A,c}$ with house temperature in normal conditions $T_{A,n}$ and outdoor temperature T_O .

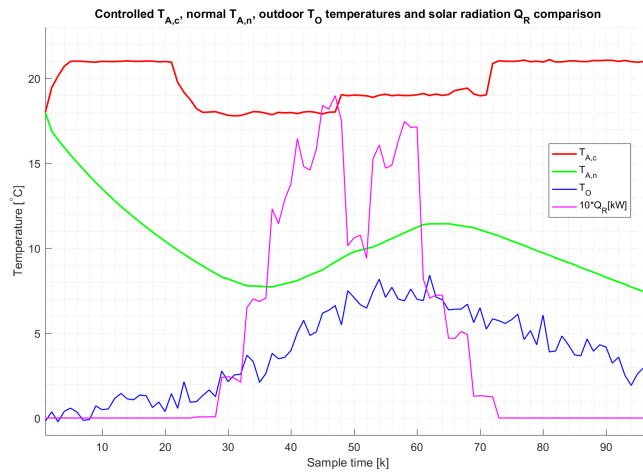


(b) Power flows of the different systems within the GSHS at each sample k .

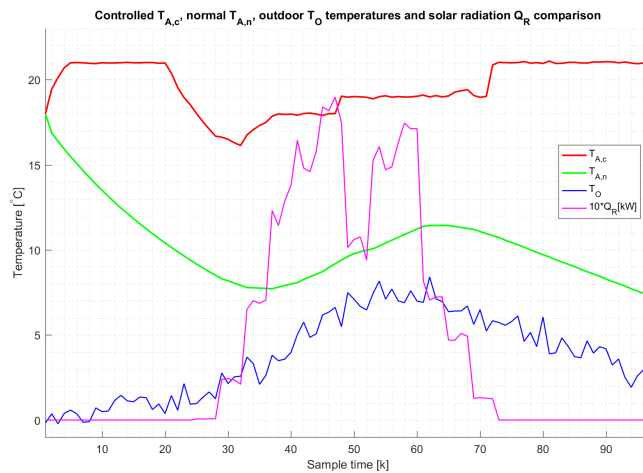
Figure 4.7: Battery example: Power and temperature performances of the system.

4.3 Scenario Comparison

Along this section a scenario comparison is presented in order to highlight some improvements regarding minimization of fossil fuel usage. Furthermore, the purpose of this example is to show the trade-off between discomfort and backup generator usage when using MPC. Such that, in *Scenario 1* there is a need to keep the house temperature near the reference while *Scenario 2* focuses on minimizing fossil fuel usage. These scenarios were built using the same weather data (forecast and real), initial battery (5 kWh) and reference temperature T_{ref} , as defined in 4.1).



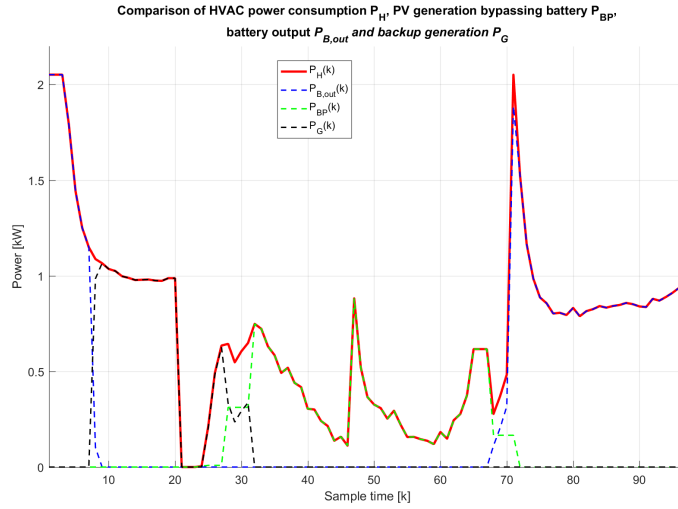
(a) Scenario 1



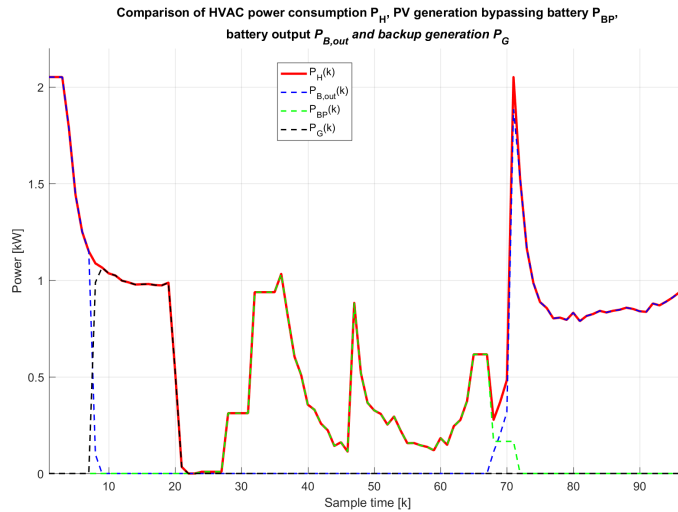
(b) Scenario 2

Figure 4.8: Scenario comparison showing the temperature trade-off.

Further, by comparing Figures 4.8a and 4.8b it can be observed that the house temperature $T_{A,c}$ in *Scenario 1* strictly follows the reference temperature while in *Scenario 2* there is a significant drop in temperature to 16°C around sample 25. To be noted that for the lower bound on temperature $T_{A,min}$ has been reduced to 16°C in the idea of lowering backup generation. Regarding the weight factors in (4.1), in the case of *Scenario 2* the weight on temperature W_{T2} has been given a lower value than the weight W_{T1} in *Scenario 1*, such that: $W_{T2} < W_{T1}$.



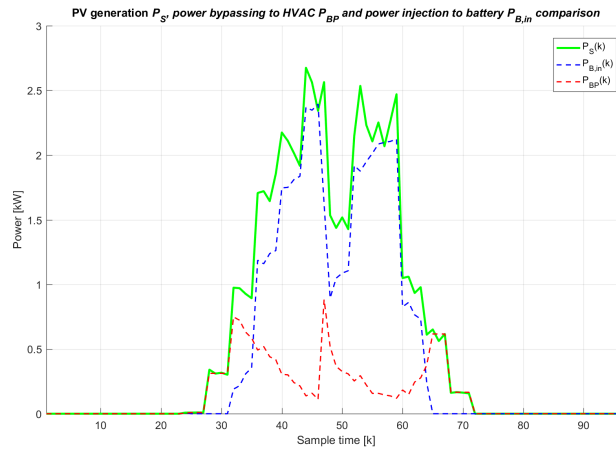
(a) Scenario 1



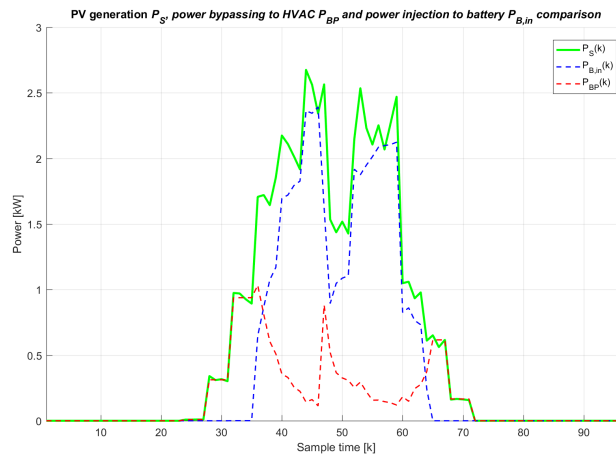
(b) Scenario 2

Figure 4.9: Scenario comparison: HVAC power consumption P_H depending on bypass power P_{BP} , power drained from battery $P_{B,out}$ and generated power P_G .

Going forward and analysing Figures 4.9a and 4.9b, it can be seen that the HVAC power demand P_H is fulfilled by the different providers in the GSHS: at first from the battery $P_{B,out}$, secondly from the backup generator P_G and last from the PV system bypassing the battery P_{BP} . Further, by comparing the backup generator power P_G it can be said that there is more generation in the case of *Scenario 1* in 4.9a as opposed to *Scenario 2* in 4.9b. In this case *Scenario 2* takes advantage of the prediction horizon ($N=20$, 5 hours ahead) and 'knows' that PV generation will kick in around sample 28, thus not using the backup generation opposed to what can be seen in *Scenario 1* for the same period.



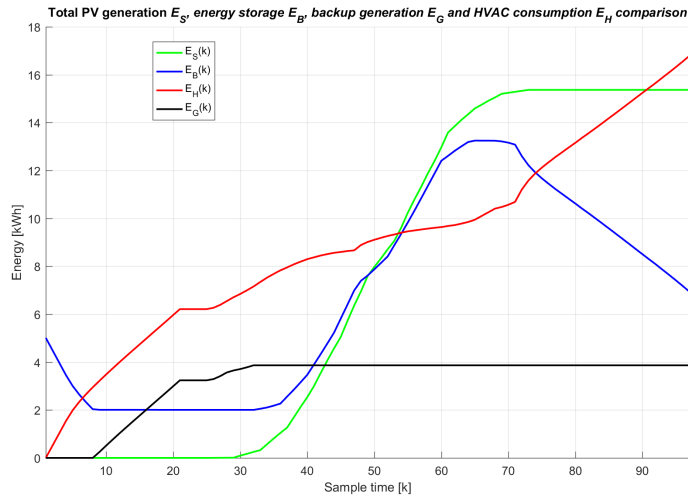
(a) Scenario 1



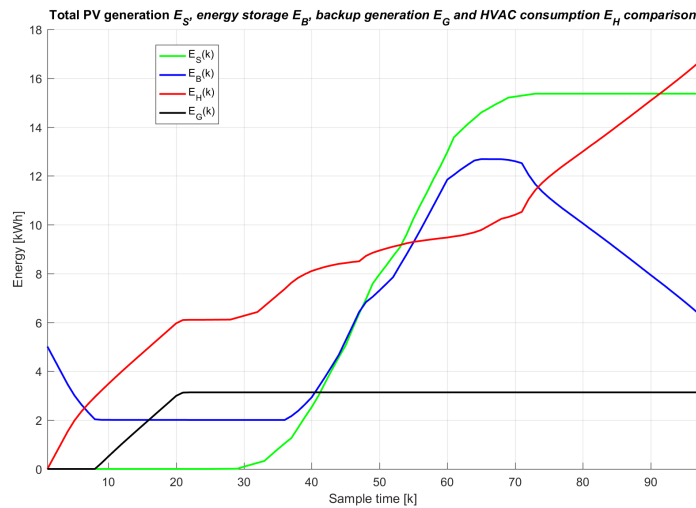
(b) Scenario 2

Figure 4.10: Scenario Comparison: PV generation P_S splitting the power to bypass P_{BP} to HVAC and power injection to battery $P_{B,in}$.

Observing Figures 4.10a and 4.10b, the PV generation P_S , bypassing P_{BP} and battery power injection $P_{B,in}$ are shown for each scenario. For *Scenario 2* there is a higher need to bypass power to the HVAC (starting from sample 30) in order to recover from the temperature deviation from the reference in 4.8b around sample 25, opposed to *Scenario 1* where the temperature $T_{A,c}$ is already to the reference. As expected, by looking at the battery output $P_{B,out}$ this is facilitated when there is no PV generation bypassing P_{BP} , while P_G is used as a last resource of power.



(a) Scenario 1



(b) Scenario 2

Figure 4.11: Scenario comparison of energy profiles within the GSHS: PV generation E_S , storage E_B , backup generator E_G and HVAC consumption E_H .

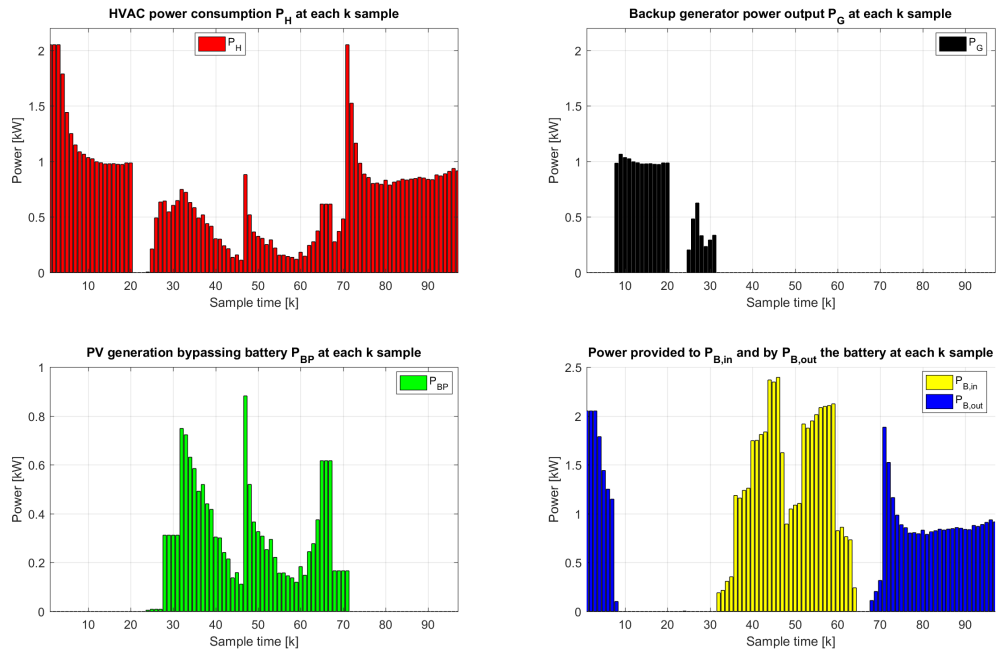
In order to compare quantitatively the two scenarios in Figures 4.11a and 4.11b the total amount of energy consumption (E_H), generation (E_S , E_G) and stored E_B can be compared. At a first glance it can be observed that the scenarios are equivalent from the perspective of the total HVAC energy consumption E_H , but the shape differs since consumption was moved later when PV generation was available. This can be seen starting from sample 30 when the energy generation E_S commenced. Further, it can be examined that in both scenarios the battery level reaches its lower bound $E_{B,min}$ around sample 20 as defined in the constraints to safeguard the battery. Moreover, due to the recovery need in *Scenario 2* the battery charging starts later at sample 36, opposed to *Scenario 1* which occurs at the beginning of sample 32 providing an extra 0.5 kWh seen clearly by looking at sample 65. Last but not least, regarding the backup energy E_G it can be observed that there is a difference of almost 1 kWh meaning that *Scenario 2* would save around a quarter more fossil fuels than *Scenario 1* in this specific day.

A different perspective of all the power flows in the system is shown in Figures 4.12a and 4.12b. Thus, comparing the battery output $P_{B,out}$ one can see that in both scenarios they are the same, however in the case of input power $P_{B,in}$ in *Scenario 1* this occurs earlier at sample 32 than its counter part at sample 36. Furthermore, by taking a look at the HVAC consumption P_H in the case of *Scenario 2* it can be seen how some of the consumption was moved to later samples when PV generation P_{BP} was available. Concluding on the backup power generation P_G it can be seen more clear that the system in *Scenario 2* is producing less than the one in *Scenario 1*, consequently consuming less fossil fuels.

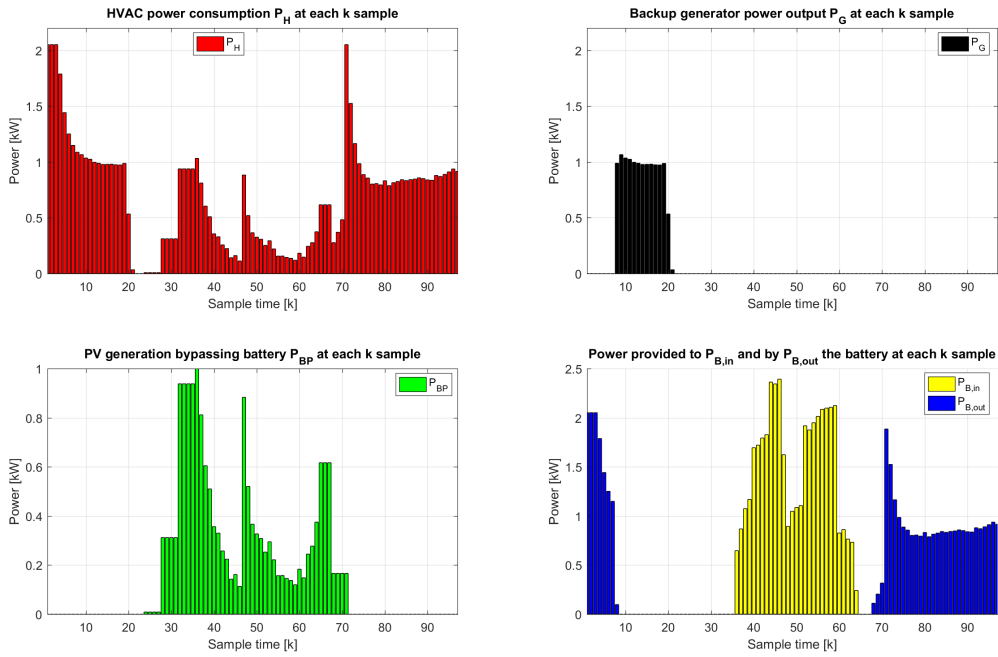
In conclusion, in this comparison it has been shown how a trade-off between temperature and backup generation has been achieved without too much comfort being expended. Such that, Table 4.2 it can be seen clearly the benefits in the case of *Scenario 2*, where on the bright side less HVAC consumption E_H (-0.5 kW) and power generation E_G (-1 kW) is made, but having a bit less battery E_B (-0.2 kW), in this particular day. Moreover, a positive result has been accomplished towards minimizing the backup generation (reducing fossil fuel usage), hence *Scenario 2* used less backup generation than *Scenario 1*.

Case	E_S [kW]	E_H [kW]	E_B [kW]	E_G [kW]
Scenario 1	15.5	17	6.9	4
Scenario 2	15.5	16.5	7.2	3
$S_2 - S_1$	0	-0.5	-0.2	-1

Table 4.2: Difference between Scenario 1 and Scenario 2 (*approximated values), showing the benefits of Scenario 2 with less consumption E_H and power generation E_G , but a bit less battery charge E_B .



(a) Scenario 1



(b) Scenario 2

Figure 4.12: Power profiles of GSHP showing battery usage $P_{B,in}$ and $P_{B,out}$, PV generation bypassing P_{BP} , backup generator P_G and HVAC consumption P_H .

Chapter 5

Conclusion

At first, a house dynamic model with heating system (HVAC) has been built based on a reduced thermal heat flow circuit. This model has been verified with a similar one implemented in well-known simulation tool used for academic research, GridLAB-D [19]. Additionally, PV system and energy storage models have been taken into account. These along with the house model and backup generation compose the green smart house system (GSHS) which can be seen in Figure 3.4.

Furthermore, the optimization problem of the GSHS has been formulated in the context of model predictive control (MPC). The implementation of the MPC problem has been achieved using Matlab in conjunction with the CVX plug-in. Moreover, the implemented MPC has proven worthy through simulations, thus providing optimal inputs to the system with respect to its dynamics, initial conditions, constraints and weather forecast. This solution has shown in the simulations that it integrates harmoniously all the GSHS components, a block diagram is provided in Figure 3.4. Also, it has proven that it can minimize fossil fuels consumption by scheduling house heating in an interval where PV generation is available instead of using backup generation. This was done without expending too much inhabitants comfort, thus making the MPC implementation a practical solution.

Further work can be made in this direction by building a more complex house, HVAC system and/or backup generator model. Another step can be taken by including other household appliances, for example water heater, dishwasher and washing machine. Additionally, house illumination and human disturbances may be added to the system. Also, other control strategies may be studied, implemented and compared with the current results. After concluding this master programme and thesis, a scientific article based on the study at hand may be pursued for publishing within a control conference.

At the beginning of this study a great amount of time was spent for pursuing a more complex house model, but had to be abandoned since it was too time consuming and would have been more difficult to integrate with the other compo-

nents of the system. This was overcome by implementing the current house model which is more limited than the one approached initially. Moreover, integrating all the components of the GSHS and making them work together was a bit of a challenge since they are diverse.

In conclusion, to my best knowledge and literature review up until the point of writing this work, such an approach has never been done before. Such that, it makes somewhat an original contribution on how to integrate and control the different systems in a green smart houses. Moreover, in this study different subjects in the area of control and automation have been approached, such as modeling of different systems and optimization through the implementation of MPC.

Bibliography

- [1] Alessandro Agnetis et al. "Load Scheduling for Household Energy Consumption Optimization". IEEE Transactions on Smart Grid 4.4: 2364-2373. 2013.
- [2] Benjamin Biegel et al. "Smart Grid Dispatch Strategy for ON/OFF Demand-Side Devices". 2013 European Control Conference. 2013.
- [3] F.A. Qayyum et al. "Appliance Scheduling Optimization in Smart Home Networks". IEEE Access 3: 2176-2190. 2015.
- [4] Mario Vařak et al. "Model predictive control of heating and cooling in a family house". MIPRO, 2011 Proceedings of the 34th International Convention. 2011.
- [5] Nuri Gökmen et al. "Investigation of wind speed cooling effect on PV panels in windy locations". Renewable Energy 90, 283-290. 2016.
- [6] Rasmus Pedersen et al. "DiSC: A Simulation Framework for Distribution System Voltage Control". Control Conference (ECC), 2015 European. IEEE. 2015.
- [7] Raymond A. de Callafon et al. "Scheduling of Dynamic Electric Loads using Energy Storage and Short Term Power Forecasting". Control Applications (CCA), 2016 IEEE Conference on. 2016.
- [8] Tom Søndergaard Pedersen et al. "Using Heat Pump Energy Storages in the Power Grid". Control Applications (CCA), 2011 IEEE Conference on. 2011.
- [9] Horst Bessai. "MIMO Signals and Systems". Springer. 2006.
- [10] S. P. Boyd and L. Vandenberghe. "Convex Optimization". Cambridge University Press. 2004.
- [11] International Code Council. "International Energy Conservation Code". <http://energycode.pnl.gov/EnergyCodeReqs/index.jsp>. 2009.
- [12] Energinet.dk. "Guidance on extensions of solar systems covered by annual netting". www.energinet.dk. 2015.
- [13] P. Gilman. "SAM Photovoltaic Model Technical Reference". National Renewable Energy Laboratory. 2015.
- [14] M. Grant and S.P. Boyd. "CVX: Matlab software for disciplined convex programming". <http://cvxr.com/cvx/>. 2017.

- [15] Mahmoud Kassas. "*Modeling and Simulation of Residential HVAC Systems Energy Consumption*". *Procedia Computer Science* 52: 754-763. 2015.
- [16] Nathaniel O. Keohane and Sheila M. Olmstead. "*Markets and the Environment*". Springer. 2016.
- [17] Pacific Northwest National Laboratory. "*GridLAB-D: Climate guide*". http://gridlab-d.sourceforge.net/wiki/index.php/Climate_Guide. 2017.
- [18] Pacific Northwest National Laboratory. "*GridLAB-D: Residential module user's guide*". http://gridlab-d.sourceforge.net/wiki/index.php/Residential_User_Guide. 2017.
- [19] Pacific Northwest National Laboratory. "*GridLAB-D Software*". <http://www.gridlabd.org/>. 2017.
- [20] S. P. Boyd M. Grant and Y. Ye. "*Global Optimization: From Theory to Implementation*". Springer. 2006.
- [21] J. Maciejowski. "*Predictive control with constraints*". Prentice Hall. 2000.
- [22] J.S. Seem. "*Modelling of heat transfer in buildings*". University of Wisconsin - Madison. 1987.
- [23] K. Gowri Z.T. Taylor and S. Katipamula. "*GridLAB-D Technical Support Document: Residential End-Use Module Version 1.0*". Prepared for U.S. Department of Energy. 2008.

Appendix A

CVX-Matlab Implementation

Implementation of GSHS models and MPC optimization using CVX and Matlab:

```
%% description
% title: MPC implementation of gshs optimization problem
% author: Robert Popescu
% group: CA1033
% Aalborg University

%% parameters and run optimization
clear all; close all; clc;
TA0 = 18;          % initial/current house air temperature
TM0 = 18;          % initial/current house mass temperature
EB0 = 0.25*20*10^3; % initial/current battery level
WT = 0.7;          % weight on house temperature – comfort
WG = 0.002;        % weight on using backup generator
WB = 0.001;        % weight on using the battery

%% csv weather (forecast) data input from gridlabd
data = csvread('data3.csv', 9, 1); % read csv file
Ta = data(:,1);    % air temperature
Tm = data(:,2);    % mass temperature
To = data(:,3);    % outdoor temperature
Qr = data(:,5);    % solar radiation
Ib = data(:,6);    % solar irradiance beam
% Ib = zeros(length(Ib),1); % for no battery and no PV scenario

%% 'real' weather by adding deviations to the predicted weather
rng(123123);      % random number generator seed
To_real = (1+randn(length(To),1)/49).*To;% 'real' outdoor temperature
```

```

Qr_real = (1+randn(length(Qr),1)/19).*Qr;% 'real' solar radiation
Ib_real = (1+randn(length(Ib),1)/19).*Ib;% 'real' solar irradiance

%% gshs parameters
Ts = 0.25;          % sampling time 15min = 1hour/4
Ua = 566;          % house air conductance
Ca = 2.290*10^6;   % house air capacitance
Um = 9889;         % house mass conductance
Cm = 9.286*10^6;   % house mass capacitance
COP = 3.5;         % hvac coef of performance
A_pv = 45;         % PV area
e_pv = 0.2;        % PV efficiency
e_d = 0.99;        % battery drain efficiency rate
e_in = 0.99;       % battery charging efficiency
e_out = 1.01;      % battery discharging efficiency

%% house state-space model
A = [-(Ua+Um)/Ca Um/Ca; Um/Cm -Um/Cm];
B = [COP/Ca 0 Ua/Ca; 0 1/Cm 0];
C = [1 0; 0 1];
gsh = ss(A, B, C, 0, 'StateName', {'Ta' 'Tm'}, ...
        'InputName', {'Ph' 'Qr' 'To'});
gshd = c2d(gsh, Ts); % discrete state-space model
[Ad, Bd, Cd, Dd, Ts] = ssdata(gshd);

%% convex problem parameters
M = 116;          % duration of control process
N = 20;           % prediction horizon (looking 5 hours ahead)
% Tref = 21;      % reference temperature
TAmin = 18;       % minimum air temperature
TAmx = 21;        % maximum air temperature
TMmin = 18;       % minimum mass temperature
TMmx = 21;        % maximum mass temperature
EBmax = 20*10^3;  % maximum battery level
EBmin = 0.1*EBmax; % minimum battery level
PGmin = 0;        % minimum backup generation
PGmax = 3*10^3;   % maximum backup generation
PHmin = 0;        % minimum HVAC consumption
PHmax = 3*10^3;   % maximum HVAC consumption
PBin_min = 0;     % minimum power injection to battery

```

```

PBin_max = 3*10^3; % maximum power injection to battery
PBout_min = 0; % minimum power drain from battery
PBout_max = 5*10^3; % maximum power drain from battery
PBP_min = 0; % minimum bypass power
% user preference on reference temperature for 2 days
Tref = [21*ones(24,1);18*ones(24,1);19*ones(24,1);21*ones(24,1);...
21*ones(24,1);18*ones(24,1);19*ones(24,1);21*ones(24,1)];

%% defining vectors of the system parameters
Ta_sys = zeros(MN+2,1);
Tm_sys = zeros(MN+2,1);
Eb_sys = zeros(MN+2,1);
Ps_sys = zeros(MN+2,1);
Ph_sys = zeros(MN+2,1);
Pg_sys = zeros(MN+2,1);
Pbin_sys = zeros(MN+2,1);
Pbout_sys = zeros(MN+2,1);
Pbp_sys = zeros(MN+2,1);

%% initial state/condition of system
Ta_sys(1) = TA0;
Tm_sys(1) = TM0;
Eb_sys(1) = EB0;

%% running mpc with cvx plug-in
for k = 1:MN+1 %the main loop as if it is in real-time
cvx_begin quiet
variable P_H(N, 1); %hvac power consumption
variable P_Bin(N, 1); %battery input power
variable P_Bout(N, 1); %battery output power
variable P_BP(N, 1); %bypass battery
variable P_G(N, 1) %backup generator power output

expression P_S(N, 1); %PV generation
expression E_B(N, 1); %battery energy level
expression T_A(N, 1); %house air temperature
expression T_M(N, 1); %house mass temperature

%initial conditions at each time step k
T_A(1) = Ta_sys(k);
T_M(1) = Tm_sys(k);

```

```

E_B(1) = Eb_sys(k);
P_S(1) = Ps_sys(k);

OBJ = 0;
for i=1:N-1
%mpc using predicted (forecast) weather data Qr, To, Ib
T_A(i+1) = Ad(1,1)*T_A(i) + Ad(1,2)*T_M(i) + ...
          Bd(1,1)*P_H(i) + Bd(1,2)*Qr(k+i) + Bd(1,3)*To(k+i);
T_M(i+1) = Ad(2,1)*T_A(i) + Ad(2,2)*T_M(i) + ...
          Bd(2,1)*P_H(i) + Bd(2,2)*Qr(k+i) + Bd(2,3)*To(k+i);

P_S(i) = A_pv*e_pv*Ib(k+i);

E_B(i+1) = e_d*E_B(i) + (e_in*P_Bin(i) - e_out*P_Bout(i))*Ts;

OBJ = OBJ+(norm(T_A(i)-Tref(k+i), 1)*WT +P_G(i)*WG +P_Bout(i)*WB);
end

minimize OBJ;
subject to

    P_S == P_Bin + P_BP;
    P_H == P_G + P_Bout + P_BP;
    P_BP <= P_S;          %P_BP <= PBP_max;
    P_BP >= PBP_min;
    T_A <= T_Amax;
    T_A >= T_Amin;
    T_M <= T_Mmax;
    T_M >= T_Mmin;
    P_H <= P_Hmax;
    P_H >= P_Hmin;
    P_G <= P_Gmax;
    P_G >= P_Gmin;
    E_B <= E_Bmax;
    E_B >= E_Bmin;
    P_Bin <= P_Bin_max;
    P_Bin >= P_Bin_min;
    P_Bout <= P_Bout_max;
    P_Bout >= P_Bout_min;

cvx_end

```

```

cvx_status
k

% compute real gshs with 'real' values of Qr_real, To_real, Ib_real
Ta_sys(k+1) = Ad(1,1)*Ta_sys(k) + Ad(1,2)*Tm_sys(k) + ...
              Bd(1,1)*P_H(1) + Bd(1,2)*Qr_real(k) + Bd(1,3)*To_real(k);
Tm_sys(k+1) = Ad(2,1)*Ta_sys(k) + Ad(2,2)*Tm_sys(k) + ...
              Bd(2,1)*P_H(1) + Bd(2,2)*Qr_real(k) + Bd(2,3)*To_real(k);
Ps_sys(k) = A_pv*e_pv*Ib_real(k);
Eb_sys(k+1) = e_d*Eb_sys(k) + (e_in*P_Bin(1) - e_out*P_Bout(1))*Ts;

% decision variables that will be input to the real system
Ph_sys(k) = P_H(1);           % hvac consumption -> heat house
Pg_sys(k) = P_G(1);           % backup generation
Pbp_sys(k) = P_BP(1);         % pv generation bypassing battery
Pbin_sys(k) = P_Bin(1);       % battery charging
Pbout_sys(k) = P_Bout(1);     % battery discharging
end

% plotting results
run 'plot_mpc.m';

```


Appendix B

House Dynamic Model

When choosing the state-space variables of an physical system, the required number of states is typically the same to the number of energy storages [ref]. In the case of the house dynamic model the heat from the weather and heating system it is chosen to be stored by means of using a temperature variable. Hence, the heat balance equations on each of these temperature nodes are given in Equations (B.1) for the indoor air temperature T_A and (B.2) for the house mass temperature T_M .

$$\dot{T}_A(t) = \frac{1}{C_A}[-(U_A + U_M)T_A(t) + U_M T_M(t) + COP \cdot P_H(t) + U_A T_O(t)] \quad (\text{B.1})$$

$$\dot{T}_M(t) = \frac{1}{C_M}[U_M T_A(t) - U_M T_M(t) + Q_R(t)] \quad (\text{B.2})$$

B.1 Transfer Matrix

In control system theory, the transfer function of single-input single-output (SISO) systems has been generalized to multiple-input multiple-output (MIMO) systems by means of a transfer function matrix [9]. Thus, in order to observe the relation between the inputs and outputs of a linear time-invariant (LTI) system the transfer matrix must be achieved. Further, the general representation of the transfer matrix in terms of the *Laplace transform* is given in Equation (B.3), where \mathbf{Y} is a column vector of the outputs, \mathbf{G} is a matrix of the transfer functions, and \mathbf{U} is a column vector of the inputs.

$$\mathbf{Y}(\mathbf{s}) = \mathbf{G}(\mathbf{s})\mathbf{U}(\mathbf{s}) \quad (\text{B.3})$$

In the case of the house dynamics expressed in Equations (B.1) and (B.2) the inputs are the HVAC power intake P_H , outdoor temperature T_O and solar radiation Q_R whilst the outputs consists of the house air T_A and mass T_M temperatures of the

MIMO system. Furthermore, following Equation (B.3) one can write the transfer matrix of the system at hand in (B.4), where each entry in the matrix is in the form of a transfer function relating each output temperature to each of the inputs.

$$\begin{bmatrix} T_A(s) \\ T_M(s) \end{bmatrix} = \begin{bmatrix} G_{11}(s) & G_{12}(s) & G_{13}(s) \\ G_{21}(s) & G_{22}(s) & G_{23}(s) \end{bmatrix} \begin{bmatrix} P_H(s) \\ T_O(s) \\ Q_R(s) \end{bmatrix} \quad (\text{B.4})$$

Further by translating Equations (B.1) and (B.1) to the *Laplace* domain result in (B.5) and (B.6) respectively.

$$sT_A(s) = \frac{1}{C_A} [-(U_A + U_M)T_A(s) + U_M T_M(s) + COP \cdot P_H(s) + U_A T_O(s)] \quad (\text{B.5})$$

$$sT_M(s) = \frac{1}{C_M} [U_M T_A(s) - U_M T_M(s) + Q_R(s)] \quad (\text{B.6})$$

Isolating the common terms from Equations (B.5) and (B.6) is done in the form of (B.7) and (B.8). Next, the air temperature from Equation (B.7) is completely isolated in (B.9) and similar for the mass temperature T_M from Equation (B.8) is isolated in (B.10).

$$T_A(s) \left[s + \frac{(U_A + U_M)}{C_A} \right] = \frac{U_M}{C_A} T_M(s) + \frac{COP}{C_A} P_H(s) + \frac{U_A}{C_A} T_O(s) \quad (\text{B.7})$$

$$T_M(s) \left[s + \frac{U_M}{C_M} \right] = \frac{U_M}{C_M} T_A(s) + \frac{1}{C_M} Q_R(s) \quad (\text{B.8})$$

$$T_A(s) = \frac{\frac{U_M}{C_A} T_M(s) + \frac{COP}{C_A} P_H(s) + \frac{U_A}{C_A} T_O(s)}{s + \frac{(U_A + U_M)}{C_A}} \quad (\text{B.9})$$

$$T_M(s) = \frac{\frac{U_M}{C_M} T_A(s) + \frac{1}{C_M} Q_R(s)}{s + \frac{U_M}{C_M}} \quad (\text{B.10})$$

In order to achieve the air temperature T_A transfer functions it is needed to replace the mass temperature T_M from Equation (B.10) into (B.7), thus will result in (B.11) and by re-arranging it gives rise to (B.12).

$$\begin{aligned} T_A(s) \left[s + \frac{(U_A + U_M)}{C_A} \right] \left[s + \frac{U_M}{C_M} \right] &= \frac{U_M^2}{C_A C_M} T_A(s) + \left[s + \frac{U_M}{C_M} \right] \frac{COP}{C_A} P_H(s) + \dots \\ &\dots + \left[s + \frac{U_M}{C_M} \right] \frac{U_A}{C_A} T_O(s) + \frac{U_M}{C_A C_M} Q_R(s) \quad (\text{B.11}) \end{aligned}$$

$$T_A(s) \left[s^2 + s \frac{C_M(U_A + U_M) + C_A U_M}{C_A C_M} + \frac{U_A U_M}{C_A C_M} \right] = \left[s + \frac{U_M}{C_M} \right] \frac{COP}{C_A} P_H(s) + \dots$$

$$\dots + \left[s + \frac{U_M}{C_M} \right] \frac{U_A}{C_A} T_O(s) + \frac{U_M}{C_A C_M} Q_R(s) \quad (\text{B.12})$$

Similar to the air temperature, the one can find the transfer functions regarding the mass temperature T_M shown in Equation (B.13).

$$T_M(s) \left[s^2 + s \frac{C_M(U_A + U_M) + C_A U_M}{C_A C_M} + \frac{U_A U_M}{C_A C_M} \right] = \frac{COP \cdot U_M}{C_A C_M} P_H(s) + \dots$$

$$\dots + \frac{U_A U_M}{C_A C_M} T_O(s) + \left[s + \frac{U_A + U_M}{C_A} \right] \frac{1}{C_M} Q_R(s) \quad (\text{B.13})$$

Looking at Equations (B.12) and (B.13), by isolating the outputs (T_A , T_M) from the inputs (P_H , T_O , Q_R) the transfer functions can be written in the form of (B.14) - (B.10).

$$G_{11}(s) = \frac{T_A(s)}{P_H(s)} = \frac{\frac{COP}{C_A} \left[s + \frac{U_M}{C_M} \right]}{s^2 + s \frac{C_M(U_A + U_M) + C_A U_M}{C_A C_M} + \frac{U_A U_M}{C_A C_M}} \quad (\text{B.14})$$

$$G_{12}(s) = \frac{T_A(s)}{T_O(s)} = \frac{\frac{U_A}{C_A} \left[s + \frac{U_M}{C_M} \right]}{s^2 + s \frac{C_M(U_A + U_M) + C_A U_M}{C_A C_M} + \frac{U_A U_M}{C_A C_M}} \quad (\text{B.15})$$

$$G_{13}(s) = \frac{T_A(s)}{Q_R(s)} = \frac{\frac{U_M}{C_A C_M}}{s^2 + s \frac{C_M(U_A + U_M) + C_A U_M}{C_A C_M} + \frac{U_A U_M}{C_A C_M}} \quad (\text{B.16})$$

$$G_{21}(s) = \frac{T_M(s)}{P_H(s)} = \frac{\frac{COP \cdot U_M}{C_A C_M}}{s^2 + s \frac{C_M(U_A + U_M) + C_A U_M}{C_A C_M} + \frac{U_A U_M}{C_A C_M}} \quad (\text{B.17})$$

$$G_{22}(s) = \frac{T_M(s)}{T_O(s)} = \frac{\frac{U_A U_M}{C_A C_M}}{s^2 + s \frac{C_M(U_A + U_M) + C_A U_M}{C_A C_M} + \frac{U_A U_M}{C_A C_M}} \quad (\text{B.18})$$

$$G_{23}(s) = \frac{T_M(s)}{Q_R(s)} = \frac{\frac{1}{C_M} \left[s + \frac{U_A + U_M}{C_A} \right]}{s^2 + s \frac{C_M(U_A + U_M) + C_A U_M}{C_A C_M} + \frac{U_A U_M}{C_A C_M}} \quad (\text{B.19})$$

B.2 Poles and Time Constants

Further analysis of the poles of the system may be made by finding the roots of Equation (B.20), where the coefficients of each term in (B.21)-(B.23).

$$as^2 + bs + c = 0 \quad (\text{B.20})$$

$$a = 1 \quad (\text{B.21})$$

$$b = \frac{C_M(U_A + U_M) + C_A U_M}{C_A C_M} \quad (\text{B.22})$$

$$c = \frac{U_A U_M}{C_A C_M} \quad (\text{B.23})$$

Knowing that all the parameters in Equation (B.25) are positive and that U_M is larger than U_A , thus implying that Δ is positive.

$$r_{1,2} = \frac{-b \pm \sqrt{\Delta}}{2a} \quad (\text{B.24})$$

$$\begin{aligned} \Delta &= b^2 - 4ac \\ &= \frac{(U_A + U_M)^2}{C_A^2} + \frac{U_A^2 U_M^2}{C_A^2 C_M^2} + 2 \frac{U_M(U_M - U_A)}{C_A C_M} > 0 \end{aligned} \quad (\text{B.25})$$

Now, factoring of Equation (B.20) can be done in (B.26) using the roots found in (B.27).

$$as^2 + bs + c = (s + r_1)(s + r_2) \quad (\text{B.26})$$

$$r_{1,2} = -\frac{C_M(U_A + U_M) + C_A U_M}{2C_A C_M} \pm \sqrt{\frac{(U_A + U_M)^2}{C_A^2} + \frac{U_A^2 U_M^2}{C_A^2 C_M^2} + 2 \frac{U_M(U_M - U_A)}{C_A C_M}} \quad (\text{B.27})$$

In the case of the thermal system at hand the time constants are at most important since they are directly connected with how fast the mediums cool or warm under the influence of external factors.

$$(s + r_1)(s + r_2) = \tau_1 \tau_2 \left(\frac{1}{\tau_1} s + 1\right) \left(\frac{1}{\tau_2} s + 1\right) \quad (\text{B.28})$$

$$\tau_1 = \frac{1}{r_1} \quad (\text{B.29})$$

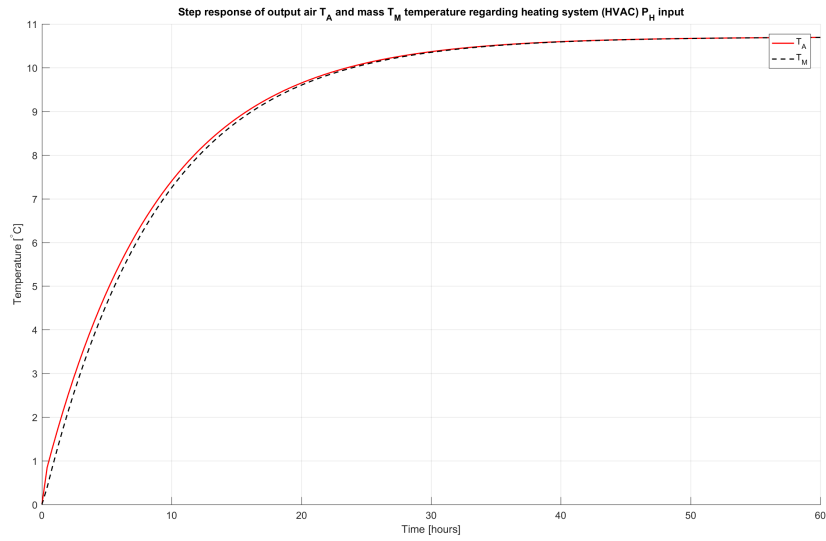
$$\tau_2 = \frac{1}{r_2} \quad (\text{B.30})$$

B.3 Step Response

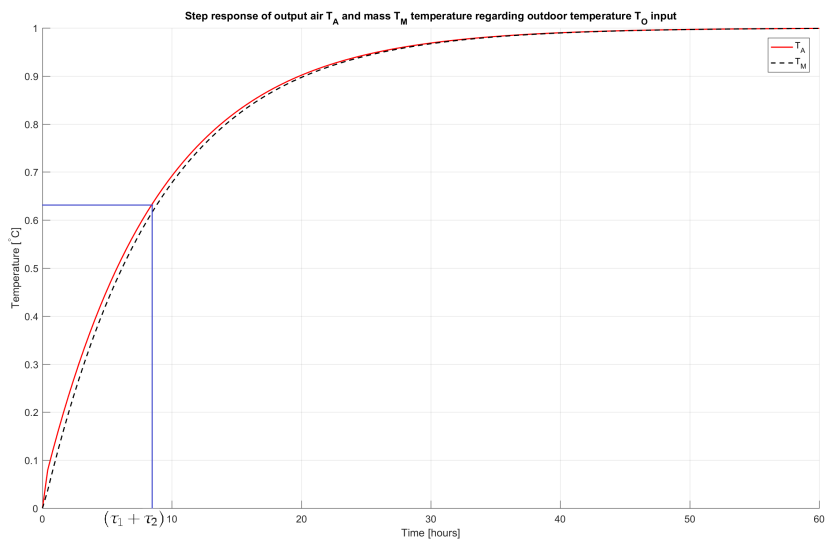
Given initial state of a system, the step response represents the time evolution of its outputs when its control inputs are Heaviside step functions as in (B.31). In control theory and other branches of engineering, the step response is the time behaviour of the outputs of a general system when its inputs change from zero to one in short time.

$$u(t) = \begin{cases} 0, & t < 0 \\ 1, & t \geq 0 \end{cases} \quad (\text{B.31})$$

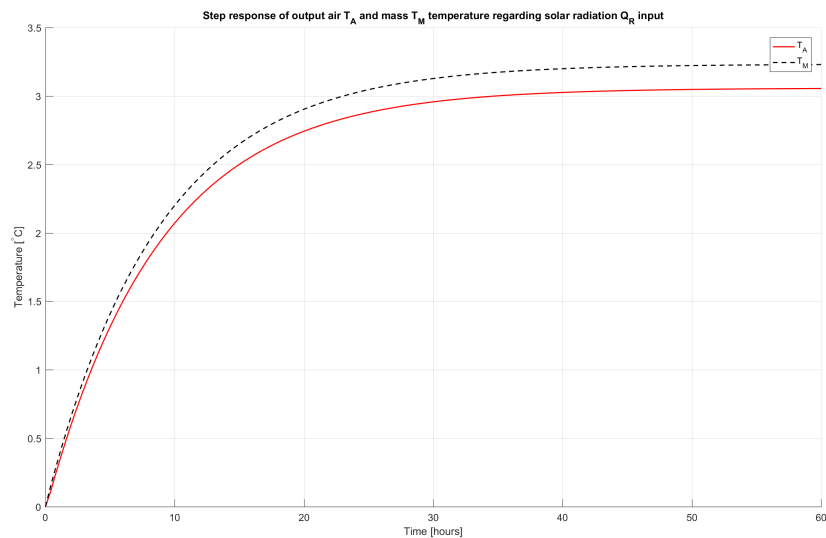
Analysis of the house dynamics is made regarding the step responses which can be seen in Figures B.1a - B.1c, where the time behaviour of the house air T_A and mass T_M temperature is observed in regards to each input of the system. To give an example on how fast does the air T_A and mass T_M temperature change in regards to the outdoor temperature T_O one may look at Figure B.1b. Moreover, it can be seen that in the case of a step increase the time constant can be found at the point where the step response reaches 63.2% of its final value (8.8) which almost equals to the time constant τ_2 plus the delay from τ_1 , found previously in (B.29) and (B.30).



(a) Air T_A and mass T_M temperatures related to 1 kW power of heating system (HVAC) P_H .



(b) Air T_A and mass T_M temperatures related to the outdoor temperature T_O .



(c) Air T_A and mass T_M temperatures related to 1 kW power of solar radiation Q_R .

Figure B.1: Step responses of air T_A and mass T_M temperatures related to each of the system inputs.